Interplay between MeCP2 and BDNF in Rett Syndrome

Inaugural-Dissertation

to obtain the academic degree

Doctor rerum naturalium (Dr. rer. nat.)

submitted to the Department of Biology, Chemistry and Pharmacy

of Freie Universität Berlin

by

CHARANYA SAMPATHKUMAR

from Chennai, India

July 2016

March 2012 - July 2016

Mentor: Prof. Dr. Christian Rosenmund

Department of Neurophysiology, Charité Medical University Berlin

Reviewer 1: Prof. Dr. Christian Rosenmund

Reviewer 2: Prof. Dr. Stephan Sigrist

Defense Date: 12 December 2016

Acknowledgements

I express my deepest gratitude to my mentor and thesis advisor, Prof. Christian Rosenmund, for giving me an opportunity to be part of his fantastic group. I would like to thank him for his tremendous support and guidance and for allowing me to work independently throughout the course of my PhD to design and perform experiments in various projects. Christian constantly encouraged me to think innovatively and challenged me intellectually by letting me question the conceptual know-how of every experiment designed as well as data interpretation with a broader perspective in mind. He has whole-heartedly been there throughout and offered me an international atmosphere comprising excellent scientists to work with.

I would like to thank Prof. Stephan Sigrist for agreeing to be my second supervisor as part of the Institute of Biology, Freie University Berlin.

I wish to thank the Helmholtz International Research School 'Molecular Neurobiology' for offering me an opportunity to be part of the PhD program affiliated to the Max Delbrueck Center for Molecular Medicine. I also wish to thank my thesis committee members, Prof. Christian Rosenmund, Prof. Erich Wanker and Dr. Thomas Mueller for their advice and support during my annual committee meetings. Many thanks to the coordinators, Dr. Michaela Herzig, Dr. Jana Droese and Annette Schledz for their constant administrative support. Further, many thanks to the MolNeuro PhD program for organizing soft skill courses and retreats as well as providing an intellectually stimulating and collaborative scientific environment over the last few years.

I am very thankful to the Collaborative Research Center SFB 665 B11 "Developmental Disturbances in the Nervous System" for funding my research.

My heartfelt thanks to all members of the Rosenmund laboratory. They have always been there to participate in discussions and support my research throughout. They have been part of my life in the last few years professionally as well as personally not only enriching my life in the lab but also for being

wonderful friends and sharing some evergreen moments. I sincerely thank every one of them.

I wish to thank my friends whose presence has enriched my life. We have had some awesome moments together and I am grateful for their unconditional support and friendship.

To my parents and my sister, Divya - I could never thank you enough. They have been with me all my life loving, caring and understanding during happy and not-so-happy moments. I would not be the person I am today without my parents' support and sacrifice and I owe them my everything. My sister has always been there with a word of encouragement and a listening ear and we have had some everlasting happy moments together. My heartfelt thanks to my family. Lastly, I want to thank Praneeth for his unconditional love, care and support ever since we met, for patiently hearing me out and understanding, and for always being there for me.

Abstract

Loss of MeCP2 function causes classic Rett syndrome, a progressive neurodevelopmental disorder. MeCP2 is a transcriptional regulator controlling transcription of a wide range of downstream target genes. Considerable evidence links MeCP2 dysfunction to a synaptic phenotype in glutamatergic neurons, leading to significant loss of synapses formed. In particular, prior studies demonstrated that altered MeCP2 levels cause abnormalities in neurite outgrowth, glutamatergic synapse formation and synaptic response. However, molecular mechanisms by which MeCP2 affects synapse formation and other morphological and functional deficits are not fully understood.

In this study, we identify a key role for BDNF in regulating glutamatergic synaptic response, general growth and differentiation in MeCP2-deficient hippocampal neurons at single-cell level. Initial analysis revealed significant reduction in axonal and dendritic outgrowth, and smaller somata in glutamatergic neurons lacking MeCP2. However, neurons overexpressing MeCP2 did not exhibit aberrant morphology suggesting that RTT-like phenotypes caused by MeCP2 loss and doubling are mediated via distinct mechanisms. Given the functional interaction between MeCP2 and BDNF, we investigated the role of BDNF signaling in regulating RTT-related morphological and physiological features in MeCP2-deficient excitatory neurons. We show, using lentivirus-mediated BDNF overexpression and exogenous application of recombinant BDNF, that increasing BDNF levels in MeCP2-deficient neurons quantitatively restored normal dendrite length, glutamatergic synapse number, soma size, and evoked EPSC amplitudes and RRP size, without affecting vesicular release efficiency. This phenotypic rescue was TrkB dependent since chronic block of TrkB receptors reverted neurons to a MeCP2-deficient state. These data elucidate the fundamental importance of BDNF-TrkB signaling for normal excitatory neuronal growth and synaptic function.

Wildtype neurons were not capable of rescuing growth deficit in neighboring MeCP2-deficient neurons in an *in vitro* RTT model as well as in female MeCP2 heterozygous mice *in vivo*. Furthermore, TrkB activation specifically in MeCP2 mutant neurons was required to reverse BDNF-driven synaptic deficit revealing a novel cell-autonomous and autocrine role for BDNF in regulating RTT phenotype. We also observed that WT and MeCP2-deficient hippocampal neurons manifest persistent BDNF fusion events indicating membrane-resident BDNF deposits, without altering overall activity-dependent BDNF secretion.

Taken together, our results demonstrate that loss of MeCP2 impairs BDNF-TrkB activity at single-cell level and that BDNF synthesis deficit and impaired cell-autonomous function of BDNF-TrkB are responsible factors for reduced excitatory synapse numbers in RTT. These findings provide mechanistic evidence for BDNF-mediated excitatory synapse formation in MeCP2 mutants and demonstrate the functional significance of a highly localized and cell-autonomous BDNF-TrkB feed-forward signaling pathway in RTT pathogenesis. This further substantiates therapeutic strategies to manipulate BDNF-TrkB signaling in MeCP2 mutant glutamatergic neurons that form 90% of all neurons in the CNS.

Zusammenfassung

Der Funktionsverlust von MeCP2 führt zu einer neurologischen Entwicklungsstörung, dem Rett-Syndrom. Der Transkriptionsfaktor MeCP2 spielt eine wichtige Rolle bei der Regulierung vieler verschiedener Zielgene. Vieles deutet auf einen Zusammenhang hin, zwischen einer Dysfunktion von MeCP2 und einem Phänotyp in glutamatergen Neuronen. Diese Dysfunktion führt zu einem signifikanten Verlust bei der Formierung der Synapsen. Verschiedene Studien konnten bereits zeigen, dass eine Veränderung der Expressionslevel von MeCP2 zu Abnormitäten bei dem Auswuchs von Neuriten, der Formierung von glutamatergen Synapsen und deren synaptischer Antwort führen. Die molekularen Mechanismen wie MeCP2 die Ausbildung der Synapsen sowie die morphologischen und funktionellen Defizite beeinflusst, sind jedoch noch nicht vollständig untersucht.

Wir konnten in dieser Studie eine Schlüsselrolle für BDNF in der Regulierung der synaptischen Antwort, dem Wachstum und der Differenzierung von hippokampalen Neuronen, welche defizient für MeCP2 waren, auf Einzelzellniveau nachweisen. Erste Analysen zeigten eine Reduktion im Auswuchs von Dendriten und Axonen. Weiterhin waren kleinere Somata in glutamatergen Neuronen, welche kein MeCP2 besaßen, sichtbar. Die Überexpression von MeCP2 zeigte jedoch keine morphologischen Veränderungen in Neuronen. Dies lässt darauf schließen, dass der Phänotyp welcher bei Rett-Syndrom beobachtet wird und in Zusammenhang mit dem Verlust oder der Verdopplung von MeCP2 Leveln in den Zellen steht, über weitere Mechanismen ausgelöst werden muss. Daraufhin untersuchten wir die Rolle von BDNF, welcher in einem funktionellen Zusammenhang mit MeCP2 steht. Durch die Überexpression von BDNF, entweder durch Infektion mit Lentiviren oder die exogene Applikation von rekombinanten BDNF, konnten wir zeigen, dass die Erhöhung der BDNF Level in Neuronen, welche kein MeCP2 besitzen, zu verschiedenen Effekten führte. Wir konnten auf quantitativem Level wieder die normale Länge der Dendriten beobachten, sowie auch die Anzahl der Synapsen in erregenden Neuronen. Ebenfalls zeigten

elektrophysiologische Messungen wieder normale evozierte EPSC Amplituden und einen normalen RRP, ohne dabei die Freisetzungswahrscheinlichkeit von Neurotransmittern zu beeinflussen. Diese Beobachtungen waren auf TrkB zurückzuführen, da die dauerhafte Blockierung von TrkB Rezeptoren zu demselben Phänotyp führten, welchen wir auch in den MeCP2 defizienten Neuronen beobachten konnten. Diese Daten erklären die fundamentale Bedeutung des Signalweges von BDNF-TrkB für das Wachstum und die synaptische Funktion von erregenden Neuronen.

In einem in vitro Rett-Modell waren benachbarte Wildtypneurone von Neuronen, welche defizient für MeCP2 waren, nicht in der Lage die morphologischen Veränderungen im Wachstum aufzuheben. Diese Beobachtung konnte in vivo bei weiblichen heterozygoten Mäusen bestätigt werden. Die Aktivierung von TrkB, insbesondere bei Neuronen von MeCP2 Mutanten, ist notwendig um die synaptischen Defizite, welche von der Fehlregulierung von BDNF ausgelöst werden, umzukehren. Dies zeigt eine neue Zell-autonome und autokrine Rolle von BDNF in der Regulierung des Rett-Phänotyps. Weiterhin beobachteten wir sowohl in WT und MeCP2 defizienten Neuronen anhaltende BDNF-Fusionen, welche auf membranständige BDNF-Depots hinweisen. Dies hatte jedoch keinen Einfluss auf die allgemeine aktivitätsabhängige BDNF Sekretion.

Zusammengefasst zeigen unsere Ergebnisse, dass ein Verlust von MeCP2 die BDNF-TrkB Aktivität auf Einzelzellebene beeinträchtigt. Defizite in der Synthese von BDNF, sowie eine beeinträchtigte Zell-autonome Funktion von BDNF-TrkB sind verantwortliche Faktoren, für eine reduzierte Anzahl von erregenden Synapsen im Rett-Model. Dies weist auf eine durch BDNF vermittelte Formierung von erregenden Synapsen in MeCP2-Mutanten hin. Weiterhin zeigt dies die funktionelle Bedeutung eines stark lokalisierten und zellautonomen BDNF-TrkB feed-forward Signalweges in der Rett-Pathogenese. Das ZNS besteht zu ca. 90 % aus erregenden Neuronen, sodass Manipulationen im Signalweg von BDNF-TrkB in MeCP2-Mutanten, bereits bestehende therapeutische Ansätze bestätigt.

Table of Contents

List of Figures

List of Abbreviations

A2bp1	ataxin 2 binding protein 1
AD	Alzheimer's disease
AKT	alpha serine/threonine protein kinase
AP	action potential
ASD	autism spectrum disorder
ATP	adenosine triphosphate
BDNF	brain-derived neurotrophic factor
BDNF-SpH	brain-derived neurotrophic factor - super ecliptic pHluorin
BSA	bovine serum albumin
$CaCl_2$	calcium chloride
CA1	*cornu ammonis* field 1 of hippocampus
Crh	corticotropin releasing hormone
CREB	cAMP response element-binding protein
dNTP	deoxynucleotide triphosphate
DAPI	4',6-diamidino-2-phenylindole
DHF	dihydroxyflavone
DIV	day in vitro
DMEM	Dulbecco's modified Eagle's medium
EGTA	ethylene glycol-bis(beta-aminoethyl ether)-N,N,N',N'-tetraacetic acid
EPSCs	excitatory postsynaptic currents
ER	endoplasmic reticulum
ERK	extracellular signal-related kinase
Fkbp5	FK506 binding protein 5
Gamt	guanidinoacetate methyltransferase
GFP	green fluorescent protein
Gprin1	G protein-regulated inducer of neurite outgrowth 1
Grm1	glutamate metabotropic receptor 1
GTP	guanosine triphosphate
HBSS	Hank's balanced salt solution
HD	Huntington's disease

HEPES	(4-(2-hydroxyethyl)-1-piperazineethanesulfonic acid)
IGF1	insulin-like growth factor-1
IPSC	inhibitory postsynaptic currents
ISI	interstimulus interval
KCl	potassium chloride
LTP	long-term potentiation
MAP2	microtubule-associated protein 2
MAPK	mitogen-activated protein kinase
MBD	methyl-CpG binding domain
MeCP2	methyl-CpG binding protein 2
Mef2C	myocyte enhancer factor 2C
MES	2-(N-morpholino)ethanesulfonic acid
$MgCl_2$	magnesium chloride
NA	numerical aperture
NBA	neurobasal media
NDS	normal donkey serum
NGF	nerve growth factor
NGS	normal goat serum
NH_4Cl	ammonium chloride
NLS	nucleus localization signal
nTS	nucleus tractus solitarius
Oprk1	opioid receptor kappa 1
PBS	phosphate-buffered saline
PBS-T	tween in phosphate-buffered saline
PI3K	phosphatidylinositol 3-kinase
PLC	phospholipase C
PPR	paired pulse ratio
PVR	probability of vesicular release
RFP	red fluorescent protein
RRP	readily releasable pool
RT	room temperature
RTT	rett syndrome
Sgk1	serum and glucocorticoid-regulated kinase 1

Syp	synaptophysin
Sst	somatostatin
TGN	transgolgi network
Tau1	isoform 1 of Tau protein
TRD	transcriptional repression domain
TrkA	tropomyosin related kinase receptor A
TrkB	tropomyosin related kinase receptor B
TX-100	triton X-100
VGLUT1	vesicular glutamate transporter 1
WT	wildtype

Chapter 1: Introduction

1.1. General overview: Synaptic transmission

The central nervous system (CNS) consists of two kinds of specialized cells: neurons and glia. Neurons are specialized structures involved in transmission of processed input information enabling information transfer and communication within the CNS. Glial cells, namely astrocytes, oligodendrocytes, ependymal cells and microglia, support the neurons.

Communication between neurons is facilitated via electrical signals within a neuron and chemical signals between neurons. Information transmission between neurons occurs at specialized points of contact called synapses (Kandel and Siegelbaum, 2000). Thus, during synaptic transmission, chemical signals called neurotransmitters are released by the presynaptic neurons upon arrival of an action potential. These neurotransmitters are stored and filled in synaptic vesicles via vesicular transporters and released into the synaptic cleft in a spontaneous or activity-dependent manner. Spontaneous fusion with the presynaptic plasma membrane occurs in a calcium-independent fashion while action potential-evoked fusion is calcium-dependent (Neher and Sakaba, 2008; Wadel et al., 2007). This fusion process triggers binding of neurotransmitters to their respective receptors in the postsynaptic neuron (Figure 1). Factors including axonal and dendritic outgrowth and arborization, and synapse number play a crucial role in affecting synaptic transmission.

Excitatory glutamatergic neurons and inhibitory GABAergic neurons predominantly form 90% of the neurons in the CNS while dopaminergic, serotonergic, cholinergic and noradrenergic neurons comprise the remaining 10%. Precise balance between the excitatory and inhibitory neurons needs to be maintained in neuronal circuits to enable proper neurotransmission. Specifically, excitation-inhibition imbalance may contribute towards pathogenesis of several neurological disorders, namely Rett syndrome which will be presented and discussed in the subsequent chapters.

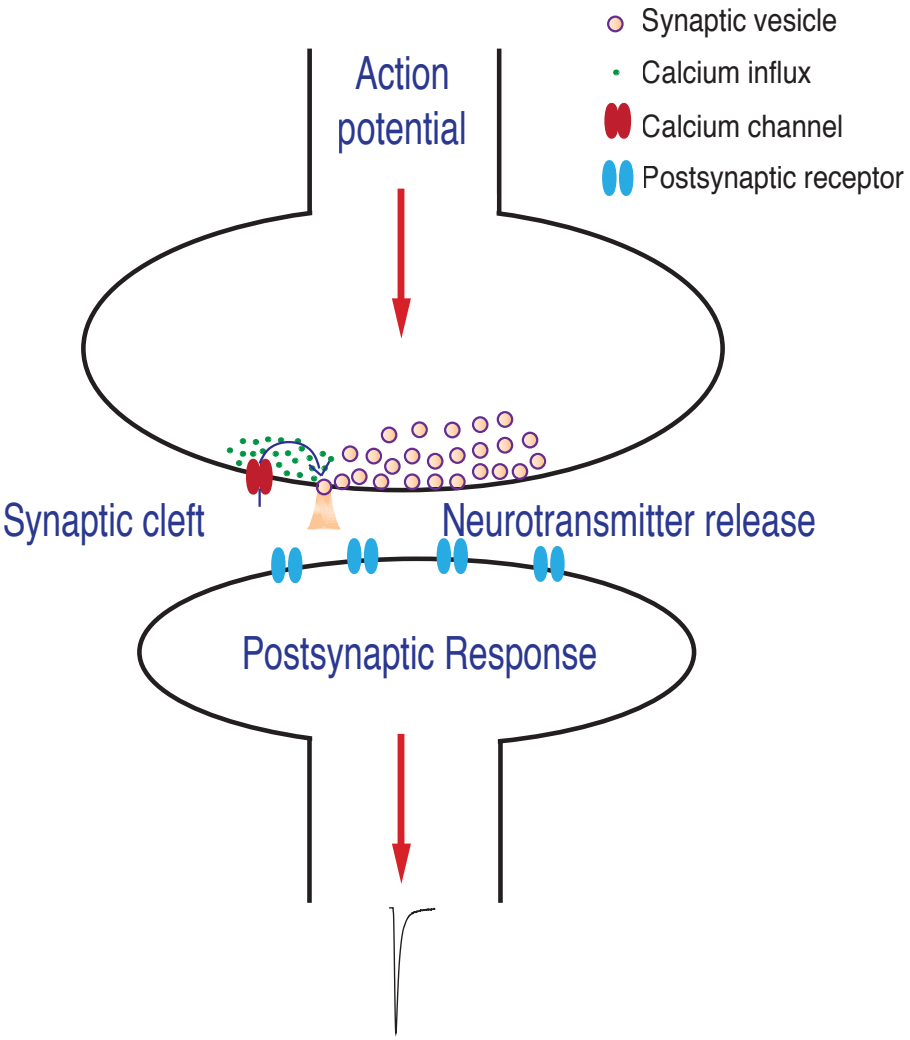

Figure 1. Basic principles of chemical synaptic transmission.
This schematic illustration demonstrates how action potential in the presynaptic neuron triggers membrane depolarization causing calcium influx via presynaptic calcium channels. Influx of calcium causes fusion of the synaptic vesicle with the presynaptic plasma membrane resulting in neurotransmitter release into the synaptic cleft. Released neurotransmitters bind to corresponding postsynaptic receptors initiating membrane depolarization of the postsynaptic neuron thereby generating information transmission across neuronal circuits.

1.2. Rett Syndrome and MeCP2

Rett syndrome (RTT) is a progressive neurodevelopmental disorder, primarily caused by mutations in the *MECP2* gene encoding the protein methyl-CpG binding protein 2 (MeCP2) (Amir et al., 1999; Wan et al., 1999; Xiang et al., 2000). *MECP2* is an X-linked gene and encodes the 486 amino acid protein MeCP2 which acts as a transcriptional regulator. RTT females are heterozygotes exhibiting somatic mosaicism for MeCP2 giving rise to two different situations: Neurons have normal MeCP2 expression when the mutated allele is found on the inactive X chromosome. On the other hand, cells are mutant if the mutated allele occurs on the active X chromosome. Two significant functional domains include the methyl CpG-binding domain (MBD) that enables MECP2 to bind to regions of DNA enriched in methylated CpG dinucleotides, and the transcriptional repression domain (TRD) that allows MeCP2 to recruit the Sin3A/histone deacetylase (HDAC) co-repressor complex resulting in chromatin compaction or loop formation as well as transcriptional repression (Nan and Bird, 2001). However, recent studies demonstrate that MeCP2 regulates a wide range of downstream target genes by both transcriptional activation and repression (Chahrour et al., 2008).

MeCP2 expression levels in the central nervous system (CNS) rise postnatally with neuronal maturation, with MeCP2 levels in human cortical neurons reaching saturation by ten years of age (Bauman et al., 1995). This progressive increase in MeCP2 levels and expression patterns with postnatal neural development indicates that MeCP2 is extremely crucial for normal neuronal growth and function.

RTT occurs with an incidence of 1 in 10,000 females and is characterized by a period of apparently normal development from 6 until 18 months of age followed by developmental regression and autistic features (Hagberg et al., 1983). Rett patients exhibit a myriad of symptoms including ataxia, seizures, anxiety, stereotypies, mental retardation, social behavioral abnormalities including lack of hand skills and impaired social interaction, lack

of communication and repetitive behaviors, respiratory abnormalities including breathing arrhythmia, and loss of motor skills resulting in deterioration in mobility (Rett, 1966). At a cellular level, RTT neurons are smaller and densely packed with altered dendritic complexity and spine number (Belichenko et al., 1997; Jentarra et al., 2010; Jiang et al., 2013; Jugloff et al., 2005). The wide spectrum of RTT symptoms associated with MeCP2 loss-of-function extends beyond classic RTT. For example, several studies have reported disrupted neurological function associated with overexpression of MeCP2 (Van Esch et al., 2005). *MECP2* duplication leading to twice the endogenous levels of MeCP2 expression is a major causal factor of mental retardation and classic RTT-like progressive neurological symptoms in males. In particular, both classic RTT as well as the MeCP2 duplication syndrome predominantly result in similar and comparable phenotypes associated with neurological disorders.

In order to further explore the role of MeCP2 in Rett syndrome, several mouse models have been generated by engineering various *MECP2* gene deletions and mutations to mimic the Rett phenotype and study neurological function at physiological levels. Specifically, mouse models for MeCP2 loss-of-function ($Mecp2^{Null/y}$) and MeCP2 overexpression ($MECP2^{Tg1}$) have been extensively studied to compare and define the pathophysiology of RTT. $Mecp2^{Null/y}$ mice grow normally until 4-6 weeks of age, after which they display RTT-like symptoms such as reduced mobility, hindlimb clasping, abnormal breathing patterns and premature death (Chen et al., 2001; Guy et al., 2001). Similarly, mice engineered to express twice the endogenous levels of MeCP2 ($MECP2^{Tg1}$) are characterized by seizures, forepaw clasping, hypoactivity, increased aggression, and around 30% die by one year of age (Collins et al., 2004; Jugloff et al., 2008; Luikenhuis et al., 2004).

These studies have illustrated comparable neurological phenotypes equivalently affecting motor function, social behavior and neural balance. Intriguingly, MeCP2 loss-of-function and overexpression features have fostered slightly different manifestations although they influence specific systems of the brain. However, these two mouse models exhibiting phenotypes similar to

respective human patients have encouraged use of these models to determine effect of MeCP2 on synaptic function and neuronal morphology.

1.3. MeCP2: Structure and Function

MECP2 is an X-linked gene spanning ~ 76 kb in the long arm of the X-chromosome (Xq28). Both human and mouse *MECP2* consist of four exons and three introns. Two different isoforms - MeCP2-e1 and MeCP2-e2 - differing in their N-termini are expressed based on alternative splicing, MeCP2-e1 being the abundant isoform (Hung and Shen, 2003; Liyanage and Rastegar, 2014). MeCP2 is distributed uniformly throughout the developing and adult brain at the mRNA and protein level, and MeCP2 is abundantly expressed in neurons comparable to histone expression. Besides the brain, MeCP2 is also widely expressed in the lung and spleen with lower expression levels in the liver, heart, kidney and small intestine (Shahbazian et al., 2002).

So far, over 200 *MECP2* mutations have been observed in RTT individuals, majority of which are found clustered within the MBD or TRD (Amano et al., 2000; Amir et al., 2000; Amir et al., 1999). Significant variations in RTT phenotypes are prevalent in patients affected by *MECP2* mutations due to somatic mosaicism and skewing of X-chromosome inactivation. In order to understand the physiological role of loss- or gain-of-function of MeCP2, electrophysiological studies have been carried out in *Mecp2*$^{Null/y}$ and *MECP2*^{Tg1} mice. Reduced and enhanced long-term potentiation (LTP) was observed in *Mecp2*$^{Null/y}$ cortical slices (Asaka et al., 2006) and *MECP2*^{Tg1} hippocampal slices (Collins et al., 2004) respectively.

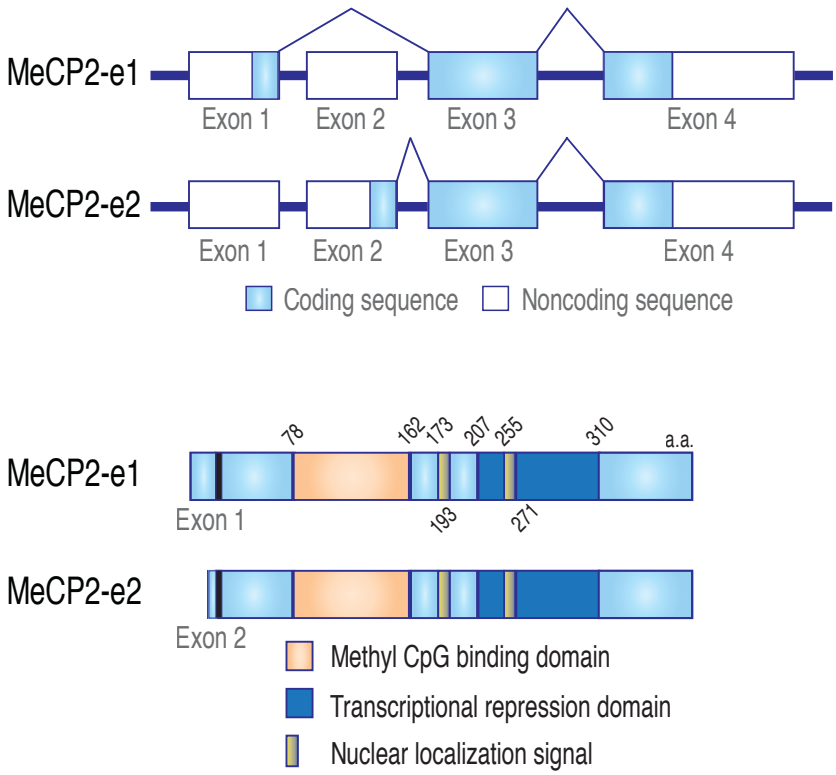

Figure 2. MeCP2 gene and protein structure.
Top panel: MECP2 consists of four exons with exons 1 and 2 subject to alternative splicing. MeCP2-e1 and -e2 are the two isoforms, MeCP2-e1 being the predominant transcript where exon 2 is excluded via alternative splicing. MeCP2-e2 is expressed at low levels in which exon 1 is excluded.
Bottom panel: MeCP2-e1 and -e2 isoforms both comprise the methyl CpG binding domain, the transcriptional repression domain and the nuclear localization signal.

At the cellular level, loss or doubling of MeCP2 reduced or enhanced the magnitude of action potential-evoked excitatory postsynaptic currents (EPSCs), respectively (Chao et al., 2007). Similarly, the readily releasable pool (RRP) was found to be correspondingly altered in *Mecp2*$^{Null/y}$ and *MECP2*^{Tg1} glutamatergic neurons. These changes in synaptic output were linked primarily to the number of glutamatergic synapses formed by these neurons (Chao et al., 2007). Morphological features associated with MeCP2 mutations have been well studied across different cell types, culture systems and brain regions. Reduced dendritic complexity with fewer dendritic branches, smaller neurons, lower spine densities, and decreased excitatory synapse number are all hallmarks of MeCP2-deficient neurons (Degano et al., 2009; Jentarra et al., 2010; Larimore et al., 2009). In congruence, *MECP2*^{Tg1} neurons show dendritic hypertrophy, increased spine densities as well as excitatory synapse number.

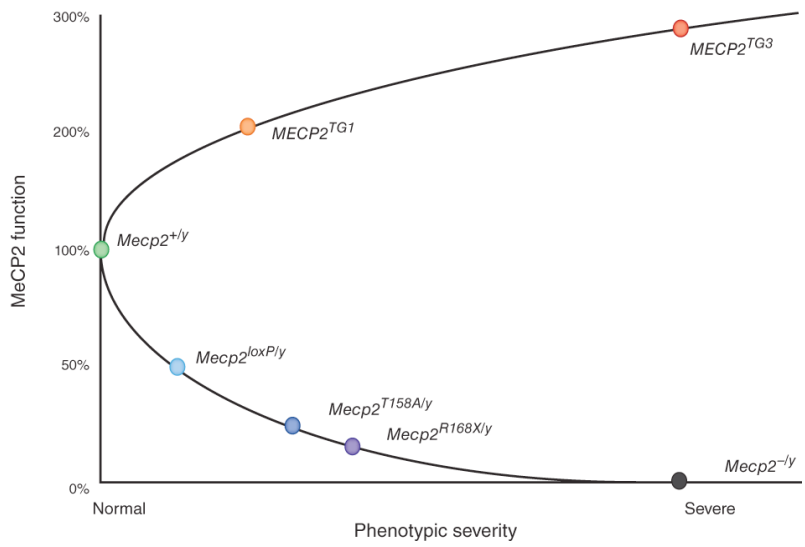

Figure 3. Phenotypic severity is altered with decreased or increased levels of MeCP2 as well as MeCP2 mutations, including *Mecp2*$^{-/y}$, *MECP2*^{Tg1}, *MECP2*^{Tg3}, *Mecp2*$^{loxP/y}$, *Mecp2*$^{T158A/y}$ and *Mecp2*$^{R168X/y}$ (taken from Chao and Zoghbi, 2012).

MeCP2 loss-of-function is also associated with decreased GABA release in inhibitory GABAergic neurons. This is indicated by reduced mIPSC amplitude and mIPSC charge in autaptic neurons as well as reduced mIPSC amplitude in cortical slices. MeCP2 was found to bind to the promoter region of *GAD1* and *GAD2* thereby affecting the production of the two GABA synthesizing enzymes (Chao et al., 2010). GABAergic neurons did not exhibit any changes in synapse formation as seen in glutamatergic neurons.

1.4. Regulation of target genes by MeCP2

An exciting element for Rett researchers has been the ability to reverse the RTT phenotype by restoring normal MeCP2 levels resulting in rescue of neurological defects associated with MeCP2 loss-of-function (Giacometti et al., 2007; Guy et al., 2007). This phenotypic rescue is controlled by causal factors including timing of activation of MeCP2 and dynamic variations in MeCP2 levels. Additionally, MeCP2 being a global transcriptional regulator of downstream target genes, advocated the search for genes regulated by MeCP2 to understand underlying molecular mechanisms, but also to identify candidates for therapeutic strategies to ameliorate the RTT disease.

Studies manipulating expression levels of MeCP2 or of target genes regulated by MeCP2 by direct and indirect mechanisms have convincingly demonstrated either reversal of the RTT phenotype or alleviation of one or more RTT features (Deogracias et al., 2012; Johnson et al., 2012; Kondo et al., 2008; Kron et al., 2014; Ogier et al., 2007; Schmid et al., 2012; Tropea et al., 2009). For example, brain-derived neurotrophic factor (BDNF) has been reported to be the most consistent MeCP2 - regulated target gene (Chahrour et al., 2008; Chang et al., 2006; Martinowich et al., 2003). Specifically, functional interaction *in vivo* between MeCP2 and BDNF has been demonstrated wherein *Bdnf* deletion from postnatal forebrain excitatory neurons of MeCP2 mutant mice resulted in an earlier onset of RTT while conditional BDNF overexpression delayed RTT onset and restored impaired spontaneous firing frequency (Chang et al., 2006).

At the single cell level, endogenous MeCP2 knockdown reduced dendrite length in E18-derived hippocampal neurons, which was specifically restored via overexpression of BDNF (Larimore et al., 2009). BDNF has been known to regulate neurite outgrowth and synapse formation in excitatory cells (Cheng et al., 2011; Finsterwald et al., 2010; Gottmann et al., 2009; McAllister et al., 1999; Park and Poo, 2013; Poo, 2001; Tolwani et al., 2002; Wang et al., 2015). Hence, it is crucial to dissect effects of BDNF regulation in MeCP2-

deficient glutamatergic neurons. Although various studies have addressed phenotypic rescue upon altered BDNF levels in MeCP2 mutant mice, underlying mechanistic pathways are not fully understood yet.

Analysis of gene expression patterns in the hypothalamus of *Mecp2*$^{Null/y}$ and *MECP2*^{Tg1} mice indicated that ~ 85% of genes were activated by MeCP2 of which the promoter regions of activated genes encoding somatostatin (*Sst*), opioid receptor kappa 1 (*Oprk1*), guanidinoacetate methyltransferase (*Gamt*), G protein-regulated inducer of neurite outgrowth 1 (*Gprin1*) and repressed genes encoding myocyte enhancer factor 2C (*Mef2c*), and ataxin 2 binding protein 1 (*A2bp1*) were specifically shown to be bound by MeCP2 (Chahrour et al., 2008). Furthermore, genes including Serum and glucocorticoid-regulated kinase 1 (*Sgk1*), FK506 binding protein 5 (*Fkbp5*) and Corticotropin releasing hormone (*Crh*) were found to be associated with RTT symptoms and enhanced in MeCP2 loss-of-function mouse models (Nuber et al., 2005). Additionally, a microarray-based global gene expression study in the cerebellum of MeCP2 knockout mice showed deregulation of several hundred genes, with twice as many activated rather than repressed (Jordan et al., 2007). A recent study performing chromatin immunoprecipitation followed by sequencing (ChIP-Seq) to elucidate specific MeCP2-gene associations indicated that interaction of MeCP2 with associated target genes was not altered upon neuronal stimulation, suggesting that MeCP2 may function specifically as a fine-tuning regulator of gene transcription (Cohen et al., 2011).

A recent study by Greenberg and colleagues correlated MeCP2-mediated neurological dysfunction to preferential disruption of long gene expression in the brain, since reduced expression of long genes attenuated RTT-associated cellular deficits in cultured MeCP2-deficient neurons and that long genes were enriched selectively for neuronal functions (Gabel et al., 2015). Similarly, *Bdnf*, Bone morphogenetic protein 4 (*Bmp4)*, *Mef2c* and Glutamate metabotropic receptor 1 (*Grm1)* promoter occupancy of mutant MeCP2 exhibiting lack of neuronal activity-induced phosphorylation (NAIP) was increased resulting in increased excitatory synaptogenesis as well as enhanced

LTP (Li et al., 2011). This may, in turn, lead to altered transcriptional regulation in the mutant hippocampus illustrating the significance of NAIP for modulating dynamic functions of the adult mouse brain. Thus, further studies addressing the role of various target genes regulated by MeCP2 will offer in-depth insight into molecular mechanisms underlying autism spectrum disorders (ASDs) and enable development of elegant therapies to correct neural dysfunction.

1.5. BDNF and TrkB

The rodent *Bdnf* gene has nine promoters, each following exon I-IX that undergo alternative splicing resulting in a large number of BDNF transcripts encoding the BDNF protein. BDNF is synthesized as a precursor protein, preproBDNF, wherein the precursor signal peptide is cleaved off to obtain proBDNF which undergoes further cleaving into the mature form of BDNF (Lessmann et al., 2003). During this process, proBDNF reaches the transgolgi network (TGN) after which it is directed towards either the constitutive or the regulated secretion pathway, via protein convertases-mediated cleaving of the prodomain in the TGN or in the vesicle lumen. The constitutive secretion pathway involves spontaneous secretion while the regulated pathway is activity-dependent and requires neural activity.

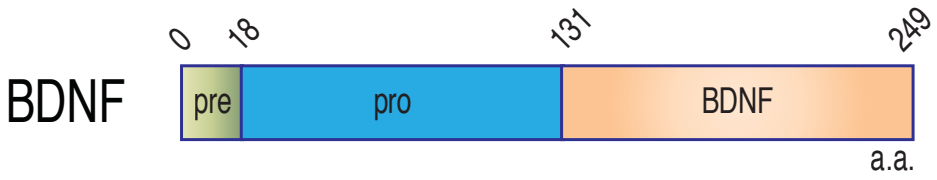

Figure 4. Primary structure of the BDNF protein.
The pre-sequence in preproBDNF is cleaved after sequestration of the full length protein into the endoplasmic reticulum (ER). The proBDNF precursor protein is further cleaved by protein convertases to obtain the mature BDNF protein.

ProBDNF and mature BDNF (mBDNF) are known to bind to specific receptors and activate downstream intracellular signaling cascades (Matsumoto et al., 2008; Woo et al., 2005; Yang et al., 2009). ProBDNF bind to the low affinity neurotrophin receptor p75 which plays a major role in apoptosis (Lessmann et al., 2003; Roux et al., 2001). Mature BDNF, on the other hand, binds to the high affinity neurotrophin receptor tropomyosin related kinase subunit B (TrkB), inducing its dimerization and autophosphorylation resulting in activation of TrkB and corresponding activation of downstream signaling pathways (Levine et al., 1998). Signaling transduction pathways that are activated upon BDNF-TrkB activation include phospholipase C ɣ (PLC ɣ) pathway that activates protein kinase C, the phosphatidylinositol 3-kinase (PI3K) pathway that activates serine/threonine kinase AKT, and the mitogen-activated protein kinase (MAPK) or extracellular signal related kinase (ERK) pathway (Mattson, 2008; Yoshii and Constantine-Paton, 2010). A major common downstream effector of all three signaling pathways is the transcription factor cAMP response element-binding protein (CREB), which is an immediate early gene and can upregulate gene expression in neurons in an activity-dependent manner.

1.6. BDNF function in neurons

BDNF is a neurotrophic factor that stimulates neurite outgrowth by propagating normal development of axons and dendrites (Yoshii and Constantine-Paton, 2010). Besides regulating basic neuronal morphology, BDNF also has crucial functions in learning and memory processes as well as in synaptic plasticity (Lu et al., 2008; Poo, 2001). BDNF and TrkB are both present in the pre- and postsynaptic sites wherein BDNF is released from both sites at synaptic and extrasynaptic loci via constitutive and activity-dependent regulated secretion (Waterhouse and Xu, 2009). BDNF acts as a highly localized signal at synapses (Kovalchuk et al., 2004) whereas it supports LTP by sustained TrkB activation via dendritic protein translation or transcription of

BDNF (Kang and Schuman, 1996). BDNF has a principal role in cognition and learning and hence extensively studied to understand its function in neurological disorders including depression, schizophrenia, bipolar disorder, Rett syndrome, and obesity-related disorders.

1.7. Role of BDNF and other neurotrophins in Neuropathology

BDNF and other neurotrophins have been known to be causal factors of several neurodegenerative and neurodevelopment disorders wherein changes in levels and activity of neurotrophins have contributed to clinical manifestations of the pathological condition. Huntingtin, whose gene mutations predominantly result in the Huntington's disease (HD), is reported to control BDNF synthesis and drive BDNF vesicles along microtubules thereby contributing to maintaining the BDNF pool in the brain; and in agreement, cultured HD cells exhibit impaired BDNF transport (Gauthier et al., 2004). Similarly, reduced BDNF production is seen in human HD cortex and studies have hypothesized that increasing BDNF levels or BDNF signaling may rescue HD phenotype (Pruunsild et al., 2007; Zuccato et al., 2001; Zuccato et al., 2008).

Besides BDNF, nerve growth factor (NGF) is known to counteract two important hallmarks of Alzheimer's disease (AD) *in vitro* and *in vivo*, *viz.* tau hyperphosphorylation and β-amyloid neurotoxicity, via regulation of amyloid gene expression and protein processing (Nuydens et al., 1997; Rossner et al., 1998; Tian et al., 2012; Zhang et al., 2010). NGF levels in serum were also found to be significantly increased in schizophrenic patients which was reduced upon 40-day clozapine treatment which implied that increased NGF levels may have a crucial role in causing schizophrenia (Ajami et al., 2014).

1.8. MeCP2 and BDNF in Rett Syndrome

Bdnf is an activity-dependent gene regulated by MeCP2 and MeCP2 is known to bind to *Bdnf* promoter IV in the absence of neuronal activity and repress *Bdnf* transcription; while upon activity, MeCP2 undergoes phosphorylation at S421, resulting in reduced binding, transcriptional derepression and increased BDNF levels (Zhou et al., 2006). Along these lines, initial studies suggested that basal *Bdnf* transcription was repressed by MeCP2 in the absence of neuronal activity in cultured neonatal cortical neurons. However, activity-dependent upregulation of *Bdnf* was unaffected in MeCP2-deficient neurons (Chen et al., 2003). This implied increased BDNF levels in the MeCP2 mutant brain in the absence of activity that may be normalized to wildtype levels upon neuronal activity. However, at the protein level, reduced BDNF levels were consistently reported across several brain regions and cell types in MeCP2 mutant mice (Chang et al., 2006; Ogier et al., 2007; Wang et al., 2006). This was later explained by reduced cortical activity in MeCP2 mutant mice which may result in overall decreased BDNF levels in mouse models associated with MeCP2 loss-of-function (Chang et al., 2006).

Pharmacological manipulation including delivery of recombinant BDNF, increasing endogenous BDNF expression or altering downstream signaling pathways are being investigated to observe RTT phenotype reversal including reversal of cardiorespiratory deficits, brainstem neuronal hyperexcitability and behavior.

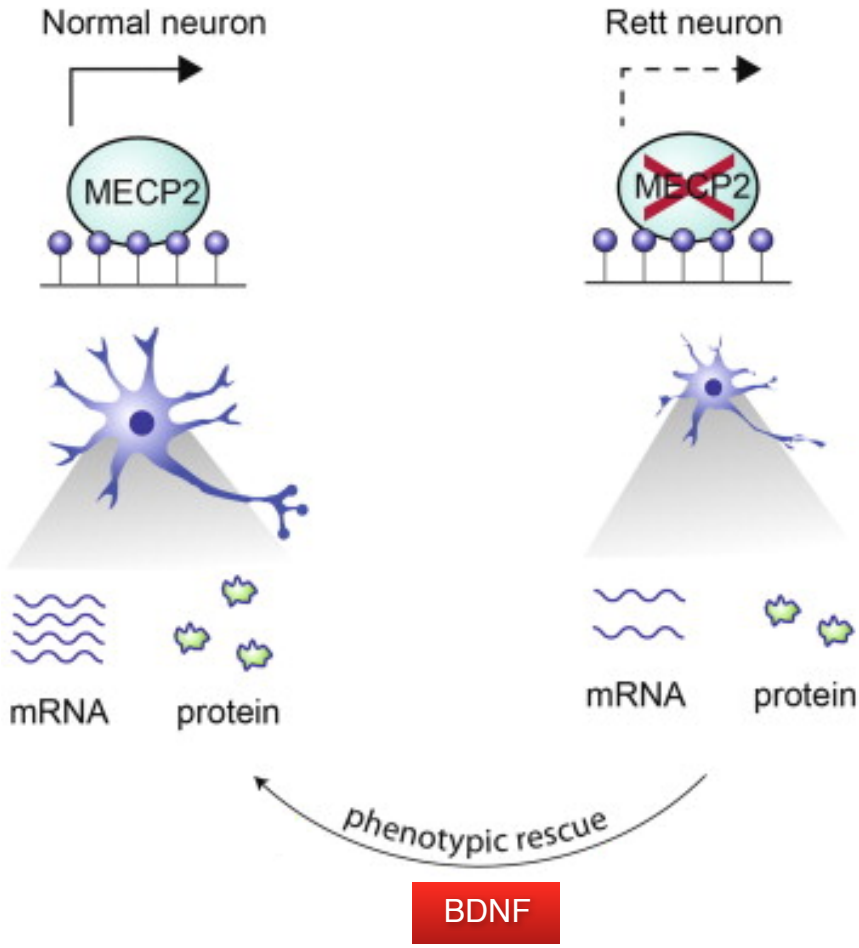

Figure 5. Scheme illustrating BDNF-mediated phenotypic rescue in MeCP2-deficient Rett neurons.
Rett-like neurons lacking MeCP2 show deficits in basic morphology, signaling cascades downstream of BDNF and overall transcription and translation. Restoring normal levels of BDNF ameliorates RTT-related deficits and results in morphological and physiological phenotypic rescue comparable to healthy wildtype neurons (modified from Wang et al., 2013).

1.9. Objectives of thesis

In this study, we examine causal molecular mechanisms affecting formation and maintenance of excitatory synapses in hippocampal neurons lacking MeCP2 at single-cell level.

(i) We characterized basic morphology of *Mecp2*$^{Null/y}$ and *MECP2*^{Tg1} autaptic neurons and found that during synaptogenesis, loss of MeCP2 reduced neurite outgrowth and neuronal soma size without affecting *MECP2*^{Tg1} neuronal morphology.

(ii) To investigate the role of BDNF signaling in *Mecp2*$^{Null/y}$ autaptic glutamatergic neurons, we manipulated BDNF levels in *Mecp2*$^{Null/y}$ neurons and discovered that increased BDNF levels quantitatively restored synaptic output and morphological phenotype in a TrkB-dependent manner.

(iii) Chronically blocking TrkB receptors resulted in a *Mecp2*$^{Null/y}$-like state, elucidating the significance of an active BDNF-TrkB pathway and normal BDNF secretion for basic growth of wildtype glutamatergic neurons in the central nervous system.

(iv) To investigate the role of BDNF-TrkB signaling in a mosaic MeCP2 expression model, we designed a WT/*Mecp2*$^{Null/y}$ co-culture *in vitro* RTT model and found that wildtype neurons are not capable of rescuing glutamatergic synapse number in neighboring MeCP2-deficient neurons.

(v) Application of TrkB agonist 7,8-dihydroxyflavone (7,8-DHF) bypassed BDNF synthesis deficiency since exogenous activation of TrkB receptors regulated normal glutamatergic synapse formation in MeCP2-deficient neurons in a mosaic expression system.

(vi) Additionally, hippocampal CA1 MeCP2-deficient neuronal nuclei were smaller than wildtype neurons in MeCP2 female heterozygous mice *in vivo,*

suggesting that autocrine BDNF secretion may play a significant role in maintaining cell-autonomy despite somatic mosaicism.

(vii) Further, we examined underlying mechanisms contributing towards the inability of WT neurons to rescue glutamatergic synapse number in neighboring *Mecp2*$^{Null/y}$ neurons in a mosaic MeCP2 expression system. We observed presence of persistent events in both wildtype and *Mecp2*$^{Null/y}$ neurons potentially due to partial deposition of BDNF on the neuronal surface, without changes in activity-dependent BDNF secretion. These data along with previous findings indicating decreased glutamatergic synapse number specifically in *Mecp2*$^{Null/y}$ neurons, illustrate impairment of a highly localized constitutive BDNF-TrkB feed-forward signaling pathway in MeCP2 mutants.

(viii) We finally asked if BDNF functions via the pre- or postsynaptic site and found that *Mecp2*$^{Null/y}$ glutamatergic synapse densities were unchanged whether formed onto a WT or *Mecp2*$^{Null/y}$ postsynaptic neuron. This demonstrated that BDNF synthesis deficiency in cultured glutamatergic neurons reduced overall synaptic output without impairing glutamatergic synaptic input.

Chapter 2: Materials and Methods

2.1. Animals

All procedures to maintain and use mice for experiments were approved by the animal welfare committee of Charité Medical University and the Berlin State government. *Mecp2*$^{Null/y}$ and *MECP2*^{Tg1} mice and their corresponding WT littermates were used for experiments involving electrophysiological and morphological studies. *Mecp2*$^{Null/y}$ mice were generated by breeding female heterozygous *Mecp2*$^{+/-}$ mice with male WT C57BLJ6/N mice while *MECP2*^{Tg1} mice were obtained by breeding female mice heterozygous for the *Mecp2* transgene to WT FVB animals.

2.2. Genotyping

2.2.1. *Mecp2*$^{Null/y}$ mice

Mecp2$^{Null/y}$ mice were genotyped for the WT (379 bp) or mutant (Het = 222 bp and 379 bp) allele.

Primers

oIMR7171 5' AAC AGT GCC AGC TGC TCT TC 3' (Common)

oIMR7172 5' CTG TAT CCT TGG GTC AAG CTG 3' (WT reverse)

oIMR7415 5' GCC AGA GGC CAC TTG TGT AG 3' (Mutant)

PCR Protocol

ddH_2O	17 µl
10x ThermoPol NEB buffer	2.5 µl
2.5 mM dNTPs	1 µl
10 µM 7171	1 µl
10 µM 7172	1 µl
10 µM 7415	1 µl
NEB Taq Polymerase	0.5 µl
Master Mix	24 µl
DNA	1 µl
Total	25 µl

Cycling parameters

Step		
1	94°C	3 min
2	94°C	30 sec
3	67°C	45 sec
4	72°C	45 sec
	Cycle back to Step 2 30 times	
5	72°C	2 min
6	4°C	forever

2.2.2. *MECP2^{Tg1}* mice

MECP2^{Tg1} mice were genotyped for the MeCP2 transgene (550 bp).

Primers

oIMR9229 5' CGC TCC GCC CTA TCT CTG A 3'

oIMR9230 5' ACA GAT CGG ATA GAA GAC TC 3'

PCR Protocol

ddH_2O	14.25 µl
10x ThermoPol NEB buffer	2.5 µl
2.5 mM dNTPs	2 µl
10 µM 9229	2.5 µl
10 µM 9230	2.5 µl
NEB Taq Polymerase	0.25 µl
Master Mix	24 µl
DNA	1 µl
Total	25 µl

Cycling parameters

Step		
1	94°C	3 min
2	94°C	30 sec
3	61°C	45 sec
4	72°C	1 min
	Cycle back to Step 2 30 times	
5	72°C	2 min
6	4°C	forever

MECP2^{Tg1} mice were also genotyped for the Y-chromosome (342 bp) to identify male animals.

Primers

YMT/2BF 5' CTG GAG CTC TAC AGT GAT GA 3'

YMT/2BR 5' CAG TTA CCA ATC AAC ACA TCA C 3'

PCR Protocol

ddH_2O	19.4 µl
10x ThermoPol NEB buffer	2.5 µl
2.5 mM dNTPs	1 µl
10 µM 2BF	0.5 µl
10 µM 2BR	0.5 µl
NEB Taq Polymerase	0.1 µl
Master Mix	24 µl
DNA	1 µl
Total	25 µl

Cycling parameters

Step		
1	95°C	5 min
2	95°C	30 sec
3	58°C	30 sec
4	72°C	1 min
	Cycle back to Step 2 29 times	
5	72°C	5 min
6	4°C	forever

2.3. Cell culture

Primary hippocampal neurons were prepared from newborn mice and plated on astrocyte feeder layers.

2.3.1. Autaptic culture system

For autaptic neuronal cultures, alkaline treated coverslips were placed in each well of culture plates and coated with 0.15% agarose (negative substrate) following which plates were coated with a cell-attachment substrate mixture consisting of 17 mM acetic acid, collagen and poly-D-lysine using a custom-made rubber stamp. This enabled astrocytes to grow only within 'islands' formed by the cell-attachment substrate. Astrocytes were derived from mouse P1 cortices by optimal trypsinization and trituration of the cortical cell suspension and plated 5-7 days before neurons.

Neurons were harvested by hippocampal dissection in cold HBSS after which hippocampi were incubated in 2 U/ml papain in DMEM at 37°C for 30-45 min. After incubation, papain was inactivated by subjecting hippocampal tissue to a prewarmed solution of albumin, trypsin inhibitor, and 5% FCS for 5 min. Following this, the inactivating solution was removed and Neurobasal-A (NBA) media containing B-27 supplement and Glutamax (Invitrogen), 50 IU/ml

penicillin and 50 μg/ml streptomycin, was added to tissue and triturated several times by repeated pipetting. Neurons were plated at 3000 cells per 35 mm well so as to obtain single neurons on isolated microislands wherein 'autapses' are formed (Bekkers and Stevens, 1991; Pyott and Rosenmund, 2002).

2.3.2. Continental culture system

To obtain continental neuronal cultures, astrocyte proliferation was arrested using the antimitotic agent 8 μM 5-fluoro-2-deoxyuridine and 20 μM uridine (FUDR) after which neurons were plated at a density of 50,000 cells per 22 mm well in NBA full media. Under these conditions, cells are evenly distributed and form processes and synapses with neighboring neurons in a network with a high degree of circuit connectivity.

2.3.3. Mixed co-culture system

For experiments involving co-culture of WT and *Mecp2*$^{Null/y}$ neurons, cells of either genotype were incubated with lentiviral constructs of interest for 1.5 h at on a rotating wheel. Following this, cells were centrifuged at 1500 rpm for 5 min twice to remove any additional viral debris. Cells were replaced with fresh NBA media and triturated by repeated pipetting for 15-20 times after which WT and *Mecp2*$^{Null/y}$ neurons were plated at a density of 14,000 cells each per 22 mm well. This procedure enabled identification of origin of synapses formed by either genotype under desired conditions.

2.4. Lentiviral constructs

Mouse cDNA constructs of pre-proBDNF, NGF and BDNF-SpH rat cDNA (kindly provided by Prof. Matthijs Verhage, Center for Neurogenomics and Cognitive Research, Amsterdam, The Netherlands) were cloned into vectors under control of the neuron-specific synapsin promoter. For co-culture experiments, we used a synapsin promoter-driven lentiviral shuttle vector expressing BDNF, cloned N-terminally to a self-cleaving T2A peptide of an

expression cassette, which harbors (i) a nuclear localization sequence-tagged green fluorescent protein (NLS-GFP) or red fluorescent protein (NLS-RFP), which was fused C-terminally via a self-cleaving P2A peptide (Kim et al., 2011) to (ii) Synaptophysin-mKate or Synaptophysin-GFP respectively (NLS-GFP-P2A-SypmKate-T2A-BDNF or NLS-RFP-P2A-SypGFP-T2A-BDNF). Control lentiviral vectors included NLS-GFP-P2A-SypmKate and NLS-RFP-P2A-SypGFP.

Lentiviral vectors and production were based on previously published protocols (Lois et al., 2002). HEK293T cells (human embryonic kidney cells) were cotransfected with 10 μg of shuttle vector and helper plasmids (pCMVdR8.9 and pVSV-G - 5 μg each) with X-tremeGENE 9 DNA transfection reagent (Roche Diagnostic). Virus-containing cell culture supernatant was harvested 72 h post transfection and purified by filtration to remove cellular debris. Filtrate aliquots were flash-frozen in liquid nitrogen and stored at -80°C. Viral titer for all rescue experiments was determined using hippocampal continental neuronal cultures. All constructs for BDNF and NGF were cloned into vectors under the control of a neuron-specific synapsin promoter. Autaptic and continental hippocampal neurons were infected with 150 μl and 75-100 μl of the viral solution (0.5-1 x 10^6 IU/ml) respectively, 24-48 h after plating. In case of co-culture experiments, WT and *Mecp2*$^{Null/y}$ neurons (200,000 cells each) were incubated with 100 μl of concentrated viral solution (1.5 x 10^7 IU/ml) and processed as described above (See 'Mixed co-culture system').

2.5. Drug treatment paradigms

Recombinant human BDNF (Promega, Madison, WI, USA) was exogenously applied to autaptic neurons at DIV 2 and added every 2-3 days at 50 ng/ml. The TrkB receptor antagonist ANA-12 (Tocris) was applied to the culture medium in which neurons were grown at DIV 6 and added at least once after 6 days or added every 3 days at 10 μM depending on culture factors including glial micro islands and neuronal growth. The BDNF neutralizing antibody α-BDNF (Millipore) was applied to the culture medium in which

neurons were grown at DIV 6 and added every 3 days at a dilution of 1:100. Neurons were treated with the TrkB agonist 7,8-dihydroxyflavone (7,8-DHF, Sigma Aldrich) at DIV 6, 9 and 12 at 500 nM.

2.6. Electrophysiology

Autaptic neurons were used for whole-cell voltage clamp experiments. Recordings were performed between days 12-17 in vitro (DIV). Postsynaptic currents were recorded from single neurons held at -70 mV with a Multiclamp 700B amplifier (Molecular Devices) under the control of Clampex 9.2 (Molecular Devices). Data sampling was done at 10 kHz and low-pass Bessel filtering done at 3 kHz. Series resistance was compensated at 70% and only cells with <12 MΩ series resistance were included. Equal number of cells per group were recorded on a given experimental day to minimize variability among datasets and data from at least two independent cultures were analyzed per experiment.

Neurons were bathed in standard extracellular solution, 300 mOsm pH 7.4, containing 140 mM NaCl, 2.4 mM KCl, 10 mM HEPES, 10 mM glucose, 2 mM $CaCl_2$ and 4 mM $MgCl_2$. The patch pipette internal solution, 300 mOsm pH 7.4, contained 134 mM KCl, 17.8 mM HEPES, 1 mM EGTA, 0.6 mM $MgCl_2$, 4 mM ATP-Mg, 0.3 mM GTP-Na, 12 mM phosphocreatine, and 50 U/ml phosphocreatine kinase. Hypertonic sucrose solution was prepared as 500 mM sucrose in standard extracellular solution (Rosenmund and Stevens, 1996).

Solutions were directly applied onto the neuron using a fast-flow micro perfusion system. Briefly depolarizing neurons from -70 mV to 0 mV for 2 ms generated an unclamped action potential that evoked excitatory postsynaptic currents (EPSC). Pulsed application of 500 mM hypertonic sucrose solution for 5 s using the fast-flow system enabled measurement of the readily releasable pool (RRP) (Rosenmund and Stevens, 1996). RRP charge was characterized by a transient inward current followed by a steady-state current which indicated the point at which rates of refilling and release were equal. Using the steady-

state current as a baseline, RRP charge was determined by integrating total area under the transient current component. Vesicular release probability (PVR) was estimated by calculating ratio of EPSC charge over RRP charge obtained from the same neuron. Paired pulse ratio was measured to study synaptic release efficiency or short-term plasticity characteristics by evoking two EPSCs with an inter-stimulus interval (ISI) of 25 ms. PPR was estimated by calculating the ratio of EPSC amplitude of second over the first synaptic response (EPSC2/EPSC1).

Data were analyzed offline using Axograph X (Axograph Scientific), Microsoft Excel and Prism (GraphPad). Unless specified otherwise, statistical significance was determined using one-way ANOVA with Tukey *post hoc* test (for three or more groups with normal distribution) or Student's *t test* (for two groups with normal distribution). In case of data not normally distributed according to D'Agostino-Pearson test, statistical significance was determined using non-parametric Kruskal-Wallis test with Dunn's *post hoc* test (for three or more groups) or Mann-Whitney *U* test (for two groups). Data was expressed as mean ± SEM Number of neurons analyzed per experiment *'n'* was indicated in the figures and 'Results' text.

2.7. Immunocytochemistry

Cultured autaptic or continental neurons were fixed at DIV 14-17 in 4% paraformaldehyde (PFA) for 15 min at room temperature (RT). Following this, neurons were washed thrice with 1x phosphate-buffered saline (PBS) solution for 10 min each. Cells were then blocked with 5% normal donkey serum (NDS) and 0.1% Tween in PBS (PBS-T) for 1.5 hours at RT. Coverslips were washed with 0.1% PBS-T thrice for 15 min each and then stained with primary antibodies of interest and incubated overnight at 4°C. Coverslips were again washed thrice with 0.1% PBS-T thrice for 15 min each and subsequently primary antibodies were labeled with secondary Alexa-Fluor 405, 488, 555 or 647 (1:500, Jackson) antibodies for 1.5 hours at RT. Post incubation, cells were washed with 0.1% PBS-T twice for 15 min each and twice with 1x PBS after

which they were mounted on glass slides with either Mowiol or ProLong Gold AntiFade reagent (Invitrogen).

Primary antibodies used included guinea pig anti-VGLUT1 (1:4000, Synaptic Systems), chicken anti-MAP2 (1:2000, Millipore), rabbit anti-MeCP2 (1:1000, Millipore) and mouse anti-Tau1 (1:1000, Millipore). MeCP2 labeling specifically involved incubation in blocking solution consisting of 5% NGS, 2% glycine, 2% BSA and 0.2% TritonX-100 (TX-100) in PBS to facilitate permeabilization of MeCP2 into the nucleus. Washing was done with 0.2% TX-100 thrice for 15 min each and secondary Alexa-555 (1:500, Invitrogen) antibody was used. Post-incubation washing and mounting was same as described above.

2.8. Quantification of neuronal morphology

16-bit images were acquired on an Olympus IX81 inverted fluorescence microscope at 20x optical magnification (numerical aperture NA = 0.75) with a CCD camera (Princeton Micromax; Roper Scientific). Morphological measurements were made using different plugins and functions in ImageJ image analysis software. For each experiment, at least two independent cultures were used for imaging and analyzing and all images were subject to uniform background subtraction (Rolling ball radius, 50 pixels) and threshold adjustment.

Morphological analysis included total axon length, dendrite length and soma area. Total dendrite length was quantified by measuring MAP2+ processes made by single neurons using the NeuronJ plugin. Total axon length was measured mainly considering Tau1+ processes. However, Tau1 also labeled proximal regions of dendrites, so we analyzed specifically Tau1+ MAP2- neurites so as to subtract overlapping processes and accurately measure axon length. Area of neuronal somata was estimated by measuring cross-sectional area across the MAP2+ cell body.

Glutamatergic synapse number was quantified in continental co-cultures. This was done by analyzing synapse density of WT and *Mecp2*$^{Null/y}$ neurons by identifying VGLUT1 and Synaptophysin+ double-labeled synapses on uniform regions of MAP2+ proximal and distal dendrites. Pre- and postsynaptic changes were studied by first identifying the genotype of neuron based on lentivirus-mediated labeling and estimating synapse density on proximal dendritic regions of identified postsynaptic neurons.

Statistical significance was determined using one-way ANOVA with Tukey *post hoc* test (for three or more groups with normal distribution) or Student's *t test* (for two groups with normal distribution). In case of data not normally distributed according to D'Agostino-Pearson test, statistical significance was determined using non-parametric Kruskal-Wallis test with Dunn's *post hoc* test (for three or more groups) or Mann-Whitney *U* test (for two groups). Data was expressed as mean ± SEM. Number of neurons analyzed per experiment *'n'* was indicated in the Figures and Results.

2.9. Immunohistochemistry

For each genotype and time point, two animals were fixed by transcardial perfusion with phosphate-buffered 4% paraformaldehyde. Coronal sections were obtained at 25 μm for 2- and 8-week old *Mecp2*$^{+/-}$ heterozygous female mice by sectioning the tissue on a Leica cryostat CM3050 S. Sections were permeabilized with 1% TX-100 for 30 min and blocked with 5% NDS, 2% glycine, 0.5% TX-100 in PBS for 30 min at room temperature after which they were incubated in mouse anti-MeCP2 (1:500, Sigma) overnight at 4°C. Sections were washed thrice with 1x PBS for 15 min each and stained with secondary Alexa 488 (1:500, Jackson) for 1 hour at RT. They were again washed thrice with 1x PBS for 15 min each and mounted on glass slides in ProLong Gold AntiFade reagent with DAPI (Invitrogen).

2.10. Quantification of hippocampal CA1 neuronal nuclei

Images were acquired on a Leica SP8 laser-scanning confocal microscope. Images were acquired at 8-bits with a 63x oil objective (NA = 1.2) at 1024 x 1024 pixel resolution. Three to four sections were imaged per animal per time point and images were acquired as z-stacks with 15-20 optical sections and maximum intensity projections were created using Fiji. Hippocampal CA1 MeCP2+ and MeCP2- neurons were identified based on their nuclear punctate staining and corresponding DAPI+ nuclei were outlined, manually traced and cross-sectional area measured using Fiji.

Statistical significance was determined using Student's *t test* (for two groups with normal distribution). In case of data not normally distributed according to D'Agostino-Pearson test, statistical significance was determined using Mann-Whitney *U* test. Data was expressed as mean ± SEM. Number of neurons analyzed per experiment *'n'* was indicated in the figures and 'Results' text.

2.11. BDNF-Superecliptic pHluorin live-cell imaging assay

Neurons were placed in standard extracellular solution as described before and 256 x 256 pixel images were acquired on an Olympus IX71 inverted microscope equipped with an Andor iXon back-illuminated CCD camera and Polychrome V illumination unit (Till Photonics) at 60x magnification (numerical aperture NA = 1.2). Data were sampled at 1 Hz.

Neurons were depolarized by KCl-induced stimulation. 60 mM KCl in standard extracellular solution was applied for 30 s using the fast flow perfusion system. Neurons were then subjected to 50 mM NH_4Cl solution for 30 s to neutralize intracellular pH and visualize all BDNF-SpH containing compartments, and 2-(N-morpholino)ethanesulfonic acid (MES)-buffered acid solution (low pH 5.5) to visualize surface-resident BDNF-SpH puncta.

BDNF-SpH fusion events were analyzed from image data stacks acquired from time-lapse recordings upon application of KCl, NH_4Cl, MES-buffered acid solution or standard extracellular solution. 4 x 4 pixel regions of interest (ROIs) were first identified and KCl-induced peak changes in fluorescence (ΔF) was normalized to initial fluorescence (F_0 = average of five frames immediately before onset of stimulus). Normalized fluorescence changes ($\Delta F/F_0$) were measured as a function of time and averaged in Axograph X (Axograph). Background fluorescence was subtracted across all image stacks using Rolling Ball function (50 pixel radius) in ImageJ and ROIs were marked to measure ΔF, using Image J. Additionally, ΔF measurements over time were baseline subtracted for each ROI per cell and averaged in Axograph X and analyzed in Prism (GraphPad). The same ROIs were used to measure changes in fluorescence (ΔF) over time upon application of NH_4Cl and MES-buffered acid solutions.

Statistical significance was determined using Student's *t test* (for two groups with normal distribution). In case of data not normally distributed according to D'Agostino-Pearson test, statistical significance was determined using Mann-Whitney *U* test. Data was expressed as mean ± SEM. Number of neurons analyzed per experiment *'n'* was indicated in the figures and Results section.

Chapter 3: Results

3.1. Loss, but not doubling of MeCP2, alters hippocampal glutamatergic neuronal morphology

We previously reported that loss or doubling of MeCP2 results in altered glutamatergic synapse number underlining tightly controlled MeCP2 dosage as a prerequisite for optimal synapse formation. However, plausible mechanisms responsible for this phenotype are not clear yet. Multiple factors including changes in neuronal growth and cell morphology could possibly contribute towards differences in glutamatergic synapse number. To address this question, we started examining the role of neurite outgrowth as a potential causal factor in hippocampal autaptic cultures derived from *MECP2*^{Tg1} and *Mecp2*$^{Null/y}$ mice. This single-cell preparation provided us a feasible system to investigate cell-autonomous mechanisms in this study.

Axonal and dendritic outgrowth was measured at DIV 2, 4, 8 and 12 from *MECP2*^{Tg1} and *Mecp2*$^{Null/y}$ glutamatergic neurons as well as control neurons derived from their respective WT littermates. Neurons were labeled for Tau1 and MAP2 so as to label for axons and dendrites respectively (Figure 6a). Analysis revealed that *MECP2*^{Tg1} neurons appeared normal and did not display any morphological deficit, with axonal and dendritic outgrowth as well as neuronal soma similar to WT neurons at DIV 2, 4, 8 and 12 (Figure 6c, 6e, 7c). In contrast, significant reduction of 41%, 38%, 28% and 23% in overall length of axons and reduction of 39%, 41%, 32% and 27% in dendritic length was seen in neurons lacking MeCP2 at DIV 2, 4, 8 and 12; respectively (Figure 6b and 6d).

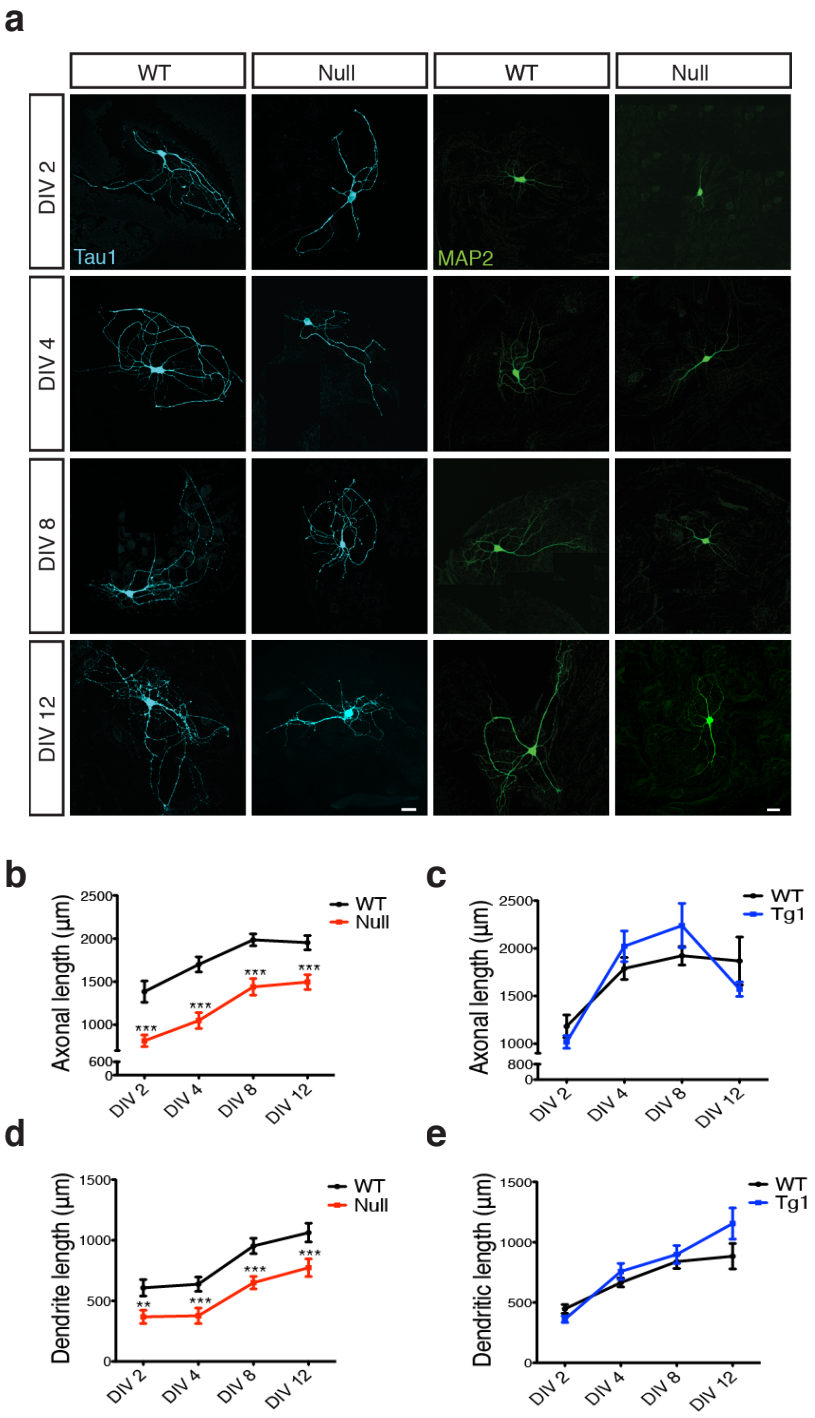

Figure 6. Loss of MeCP2 alters axonal and dendritic outgrowth.
(a) Co-immunostaining of glutamatergic hippocampal neurons from WT and *Mecp2*$^{Null/y}$ mice at DIV 2, 4, 8 and 12 for Tau1 (cyan) and MAP2 (green). Scale bars represent 20 μm. (b-e) Mean axonal length and dendritic length measured at different time points for *Mecp2*$^{Null/y}$ (b,d) and *MECP2*^{Tg1} neurons (c,e).
Data shown as mean ± SEM. **p < 0.01; ***p < 0.001.

Rett patients and mice display reduced brain size (Chen et al., 2001) and small neuronal soma (Bauman et al., 1995). In congruence, we observed a deficit in general growth and differentiation specifically in *Mecp2*$^{Null/y}$ glutamatergic neurons. We then estimated soma area and found that *Mecp2*$^{Null/y}$ somata were 24%, 32%, 30% and 33% smaller in size as compared to their WT counterparts at DIV 2, 4, 8 and 12 respectively (Figure 7a and 7b). However, *MECP2*^{Tg1} neuronal soma remained similar to that of WT (Figure 7c).

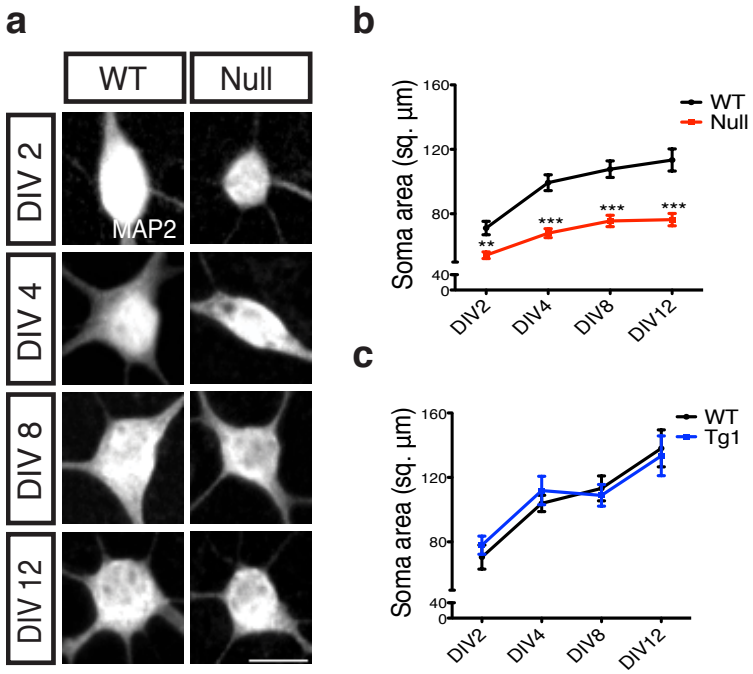

Figure 7. Loss of MeCP2 alters neuronal soma size.
(a) Somatic labeling of glutamatergic hippocampal neurons from WT and *Mecp2*$^{Null/y}$ mice at DIV 2, 4, 8 and 12 with MAP2. Scale bar represents 20 μm. (b,c) Mean soma area measured at different time points for *Mecp2*$^{Null/y}$ (b) and *MECP2*^{Tg1} neurons (c). Data shown as mean ± SEM. **p < 0.01; ***p < 0.001.

These findings show a general growth deficit in neurons lacking MeCP2 quite distinct from the *MECP2*^{Tg1} gain-of-function phenotype. Although this overall growth defect could contribute to decreased synapse number in *Mecp2*$^{Null/y}$ neurons, *MECP2*^{Tg1} neurons certainly function via an alternate mechanism to maintain enhanced synapse number implying role of other putative mechanism(s) in regulating normal synapse formation.

3.2. BDNF overexpression in *Mecp2*$^{Null/y}$ autaptic neurons restores synaptic output and basic neuronal morphology

MeCP2 is a transcriptional regulator that activates or represses expression of very many downstream genes based on cell type, origin, age and heterogeneity of brain region. Given that BDNF (i) is a consistent neuronal target gene of MeCP2, (ii) is an essential regulator of synapse formation and dendritic complexity and, (iii) levels are reduced in MeCP2 knockout mice (Chang et al., 2006); we investigated the mechanistic role of BDNF signaling in regulating synaptic output and synapse formation in *Mecp2*$^{Null/y}$ neurons at single-cell level.

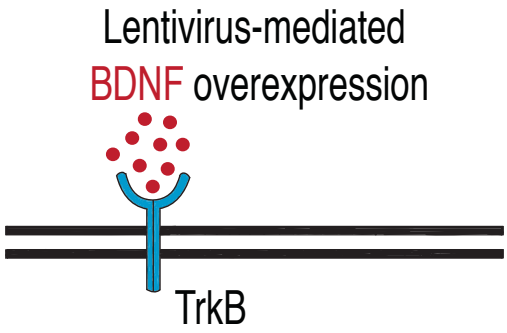

Figure 8. Experimental scheme of lentivirus-mediated BDNF overexpression in *Mecp2*$^{Null/y}$ neurons, showing neuronal membrane (black), BDNF (red) and TrkB receptor (blue).

We began investigating the role of BDNF signaling by utilizing the lentiviral system driven by a synapsin promoter to overexpress BDNF in WT and *Mecp2*$^{Null/y}$ neurons to attempt rescue of growth deficit and look for chronic effects of BDNF (Figure 8). WT and *Mecp2*$^{Null/y}$ neurons expressing GFP were used as control.

We first analyzed neuronal morphology across all experimental groups. Specifically, morphological parameters including dendrite length (WT: 1184±79.75 μm; Null: 688.2±50.16 μm, $p<0.001$; Null+BDNF: 1054±68.2 μm, $p<0.01$), excitatory synapse number (WT: 280±24.13; Null: 143±10.05, $p<0.001$; Null+BDNF: 293±39.34, $p<0.01$) and soma size (WT: 122.5±5.78 μm^2; Null: 88.09±3.71 μm^2, $p<0.001$; Null+BDNF: 125.4±6.83 μm^2, $p<0.01$) were analyzed (Figure 9a and 10a). We found that dendrite length (Figure 9b), glutamatergic synapse number (Figure 10b) and soma size (Figure 9c) in *Mecp2*$^{Null/y}$ neurons were reduced down to 58%, 51% and 72% of WT and rescued up to 89%, 105% and 102% of that of WT neurons respectively upon BDNF overexpression. These initial findings indicate that morphological deficit in *Mecp2*$^{Null/y}$ neurons was completely restored by BDNF overexpression.

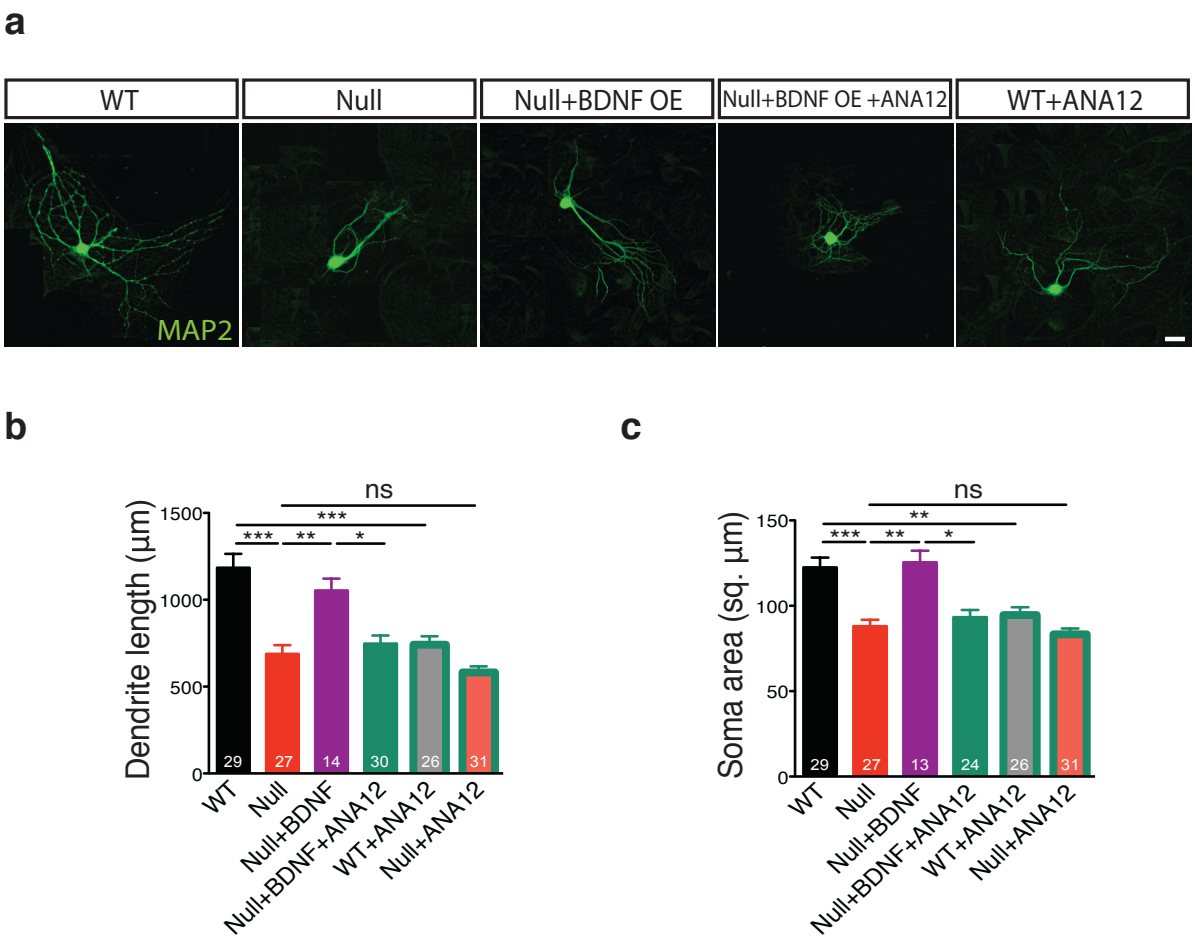

Figure 9. BDNF overexpression in *Mecp2*$^{Null/y}$ glutamatergic autaptic neurons normalizes dendrite length and soma size.

(a) Representative images of dendritic outgrowth indicated by MAP2 (green) labeling under the following conditions (from left to right): WT, Null, Null + BDNF, Null + BDNF + ANA12, WT + ANA12. Scale bar represents 20 μm. (b,c) Bar graphs show mean dendrite length (b) and neuronal soma area (c).

Number of neurons (n) shown in the bars for all graphs. Data shown as mean ± SEM. *p < 0.05; **p < 0.01; ***p < 0.001; ns: not significant.

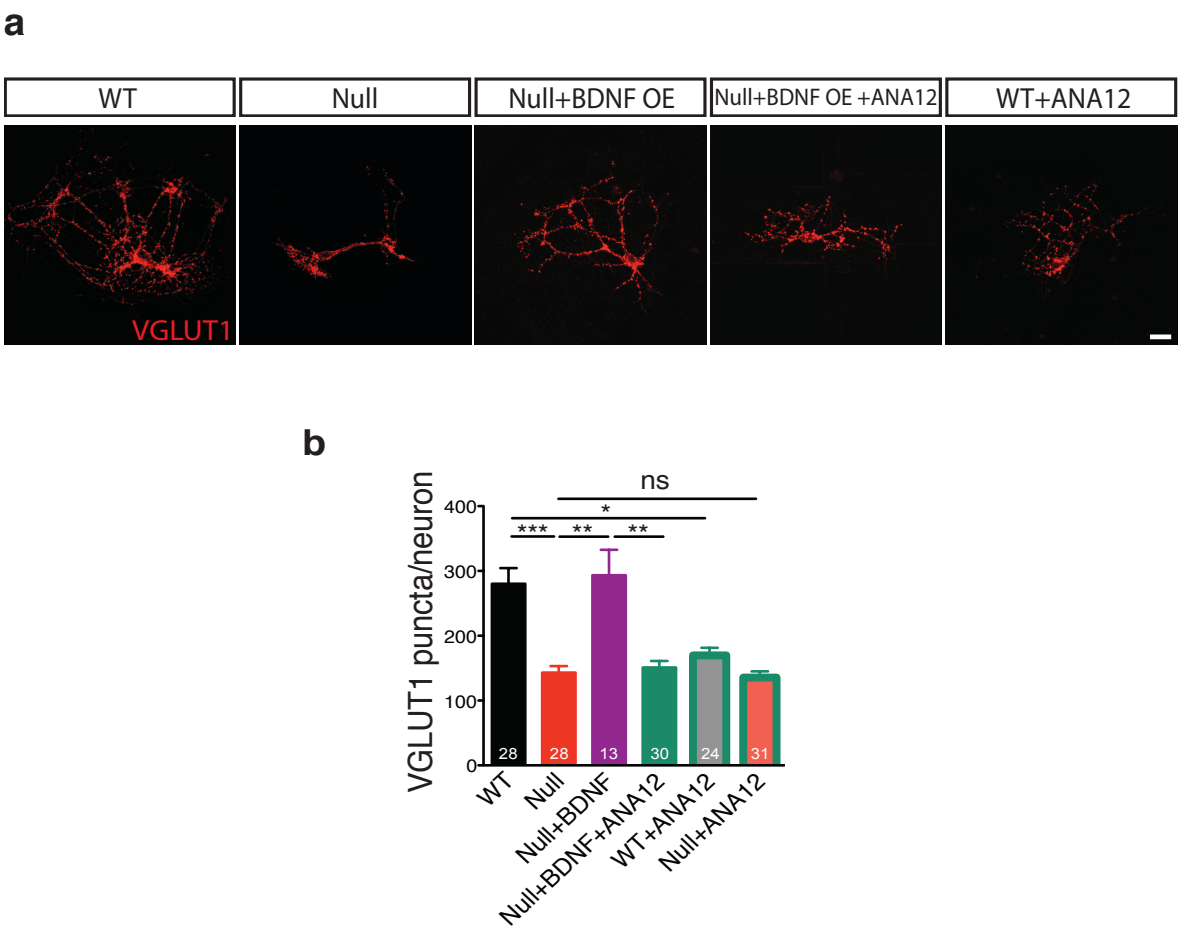

Figure 10. BDNF overexpression in *Mecp2*$^{Null/y}$ glutamatergic autaptic neurons normalizes synapse number.

(a) Representative images of glutamatergic synapses indicated by VGLUT1 (red) labeling under the following conditions (from left to right): WT, Null, Null + BDNF, Null + BDNF + ANA12, WT + ANA12. Scale bar represents 20 μm. (b) Bar graph shows mean glutamatergic synapse number.

Number of neurons (n) shown in the bars for all graphs. Data shown as mean ± SEM.

*p < 0.05; **p < 0.01; ***p < 0.001; ns: not significant.

We then examined physiological consequences of BDNF overexpression in WT and *Mecp2*$^{Null/y}$ glutamatergic neurons. For this purpose, we measured several physiological parameters including AP-dependent evoked EPSC amplitude, RRP size, paired pulse ratio (PPR) and probability of vesicle release (P_{vr}) in all experimental groups. *Mecp2*$^{Null/y}$ neurons revealed 54% decrease in evoked EPSC amplitude (2.92±0.42 nA, $p<0.05$) (Figure 11a and 11b) and 58% decrease in RRP charge (0.37±0.05 nC, $p<0.01$) (Figure 12a and 12b) as compared to WT neurons (EPSC: 6.38±0.9 nA; RRP: 0.89±0.14 nC), both of which were rescued back up to 113% and 87% of WT levels (EPSC: 7.23±0.97 nA, $p<0.01$; RRP: 0.77±0.09 nC, $p<0.01$). We observed no changes in PPR or P_{vr} measurements (Figure 12c and 12d) indicating that short-term plasticity and release efficiency characteristics remained unaffected under all conditions (with or without BDNF overexpression).

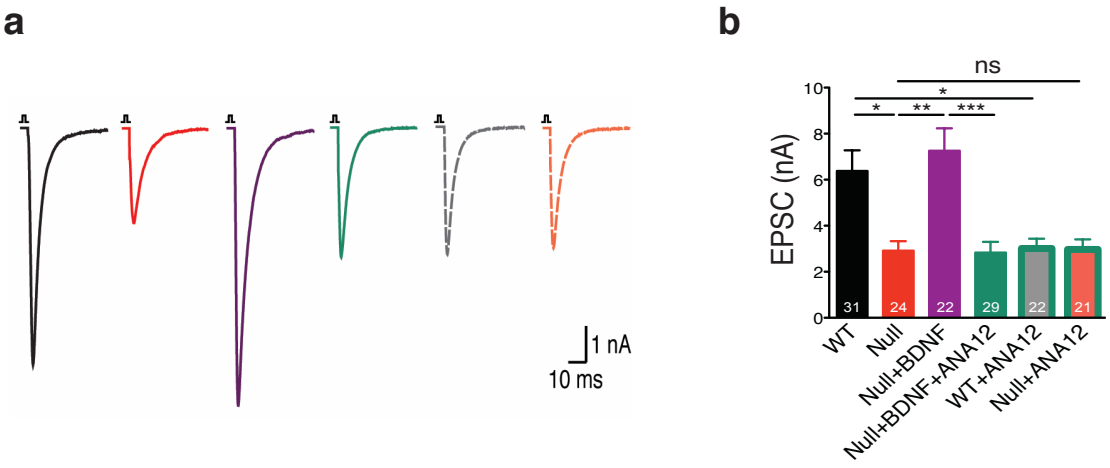

Figure 11. BDNF overexpression in *Mecp2*$^{Null/y}$ glutamatergic autaptic neurons restores evoked EPSC amplitude.

(a) Representative traces of evoked EPSCs recorded from autapses under the following conditions: WT, Null, Null + BDNF, Null + BDNF + ANA12, WT + ANA12, Null + ANA12. (b) Bar graph shows mean evoked EPSC amplitude.

Number of neurons (n) shown in the bars for all graphs. Data shown as mean ± SEM. *p < 0.05; **p < 0.01; ***p < 0.001; ns: not significant.

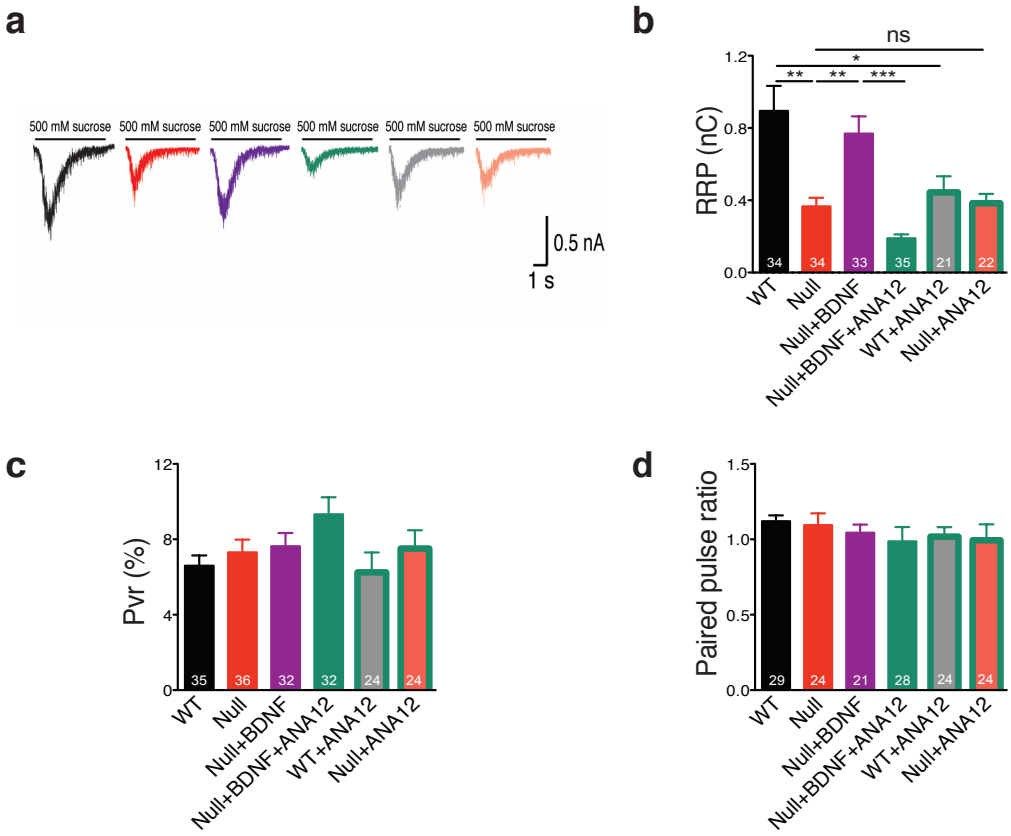

Figure 12. BDNF overexpression in *Mecp2*$^{Null/y}$ glutamatergic autaptic neurons restores readily releasable vesicle pool size without affecting vesicular release efficiency.

(a) Representative traces of average postsynaptic response to 5 s application of 500 mM sucrose recorded from autapses under the following conditions: WT, Null, Null + BDNF, Null + BDNF + ANA12, WT + ANA12, Null + ANA12. (b-d) Bar graphs show mean RRP size (b), vesicular release probability, P_{vr} (c) and paired pulse ratio, PPR, with 25 ms inter-stimulus interval (d).

Number of neurons (n) shown in the bars for all graphs. Data shown as mean ± SEM. *p < 0.05; **p < 0.01; ***p < 0.001; ns: not significant.

Furthermore, overexpressing BDNF in WT neurons failed to improve synaptic output or basic morphology indicating that the *MECP2*^{Tg1} gain-of-function phenotype was not due to increased BDNF levels (Figure 13).

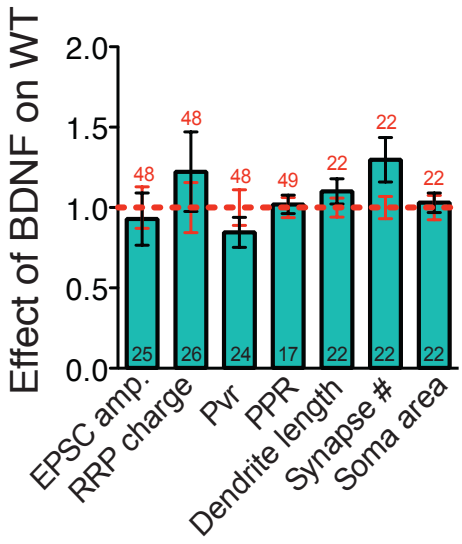

Figure 13. BDNF overexpression in WT glutamatergic autaptic neurons does not affect synaptic and morphological phenotypes.
(a) Bar graph shows EPSC amplitude, RRP size, $P_{vr,}$ PPR, dendrite length, glutamatergic synapse number and soma area, normalized to WT (dashed red line). Number of neurons (n) shown in the bars for all graphs. Number of WT neurons shown in red above the red dashed line. Data shown as mean ± SEM.

Thus, we find a major functional and morphological regulatory role for BDNF signaling in *Mecp2*$^{Null/y}$ neurons.

3.3. TrkB inactivation converts WT and rescued *Mecp2*$^{Null/y}$ neurons to a MeCP2-deficient state

Given that restoring normal levels of BDNF synthesis in MeCP2-deficient glutamatergic neurons was sufficient to rescue MeCP2 loss-of-function phenotype, we next asked if disruption of BDNF binding to TrkB could negate effects of BDNF overexpression in *Mecp2*$^{Null/y}$ neurons. The low molecular weight TrkB ligand, ANA-12, selectively binds to the TrkB receptor thereby blocking BDNF-induced TrkB activation and inhibiting intracellular signaling cascades downstream of TrkB (Cazorla et al., 2011). Post lentivirus-mediated BDNF overexpression at DIV 2, ANA-12 was applied to the culture medium at DIV 6 and DIV 11 and neurons were fixed for morphology analysis or taken for electrophysological measurements between DIV 12-16.

Synaptic output (evoked EPSC amplitude: 2.83±0.47 nA, $p<0.001$ and RRP size: 0.19±0.02 nC, $p<0.001$) as well as morphological phenotype (synapse number: 151±9.99, $p<0.01$; dendrite length: 748±46.21 μm, $p<0.05$ and soma size: 93.4±4.2 μm^2, $p<0.05$) were reverted down to *Mecp2*$^{Null/y}$ control levels, upon ANA-12 application in BDNF-overexpressing *Mecp2*$^{Null/y}$ neurons (Figure 11a, 11b, 12a, 12b). ANA-12 was also applied to WT and *Mecp2*$^{Null/y}$ glutamatergic neurons. MeCP2-deficient neurons did not show any further changes in synaptic output or morphological features upon ANA-12 application indicating strongly that the BDNF-TrkB pathway was completely disrupted in glutamatergic neurons lacking MeCP2. However, WT neurons showed a *Mecp2*$^{Null/y}$ - like deficit in synaptic output and morphological phenotype upon ANA-12 application affirming that BDNF-TrkB activity was disrupted in WT neurons upon chronically blocking TrkB receptors (Figure 11a, 11b, 12a, 12b). In all experimental groups, PPR and P_{vr} remained unchanged (Figure 12c and 12d).

These findings together illustrate the significance of a canonical BDNF-TrkB signaling pathway essential for normal growth and synapse formation in WT glutamatergic hippocampal neurons.

3.4. BDNF neutralization reverts synaptic output and synapse number back to *Mecp2*$^{Null/y}$ levels

We next specifically blocked BDNF function by treating BDNF overexpressing *Mecp2*$^{Null/y}$ neurons with an anti-BDNF neutralizing antibody, which allowed us to confirm if the physiological and morphological changes observed were indeed mediated by BDNF overexpression (Figure 14).

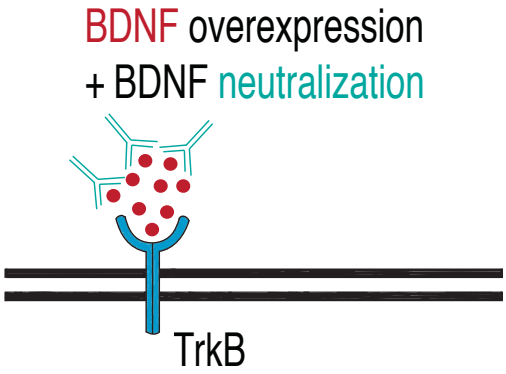

Figure 14. Experimental scheme of lentivirus-mediated BDNF overexpression and BDNF neutralization in *Mecp2*$^{Null/y}$ neurons, showing neuronal membrane (black), BDNF (red), TrkB receptor (blue) and BDNF neutralizing antibody (cyan).

BDNF neutralization led to 50% decrease in EPSC amplitude and 53% decrease in RRP size in BDNF-overexpressing *Mecp2*$^{Null/y}$ neurons as compared to WT, thereby negating phenotype rescue seen via increased expression of BDNF (Figure 15a-d). However, PPR and P_{vr} remained unaffected as before (Figure 15e and 15f). Thus, we found that abolishing BDNF function affected synaptic function in *Mecp2*$^{Null/y}$ glutamatergic neurons, further strengthening the hypothesis of normal BDNF synthesis requirement in MeCP2-deficient neurons.

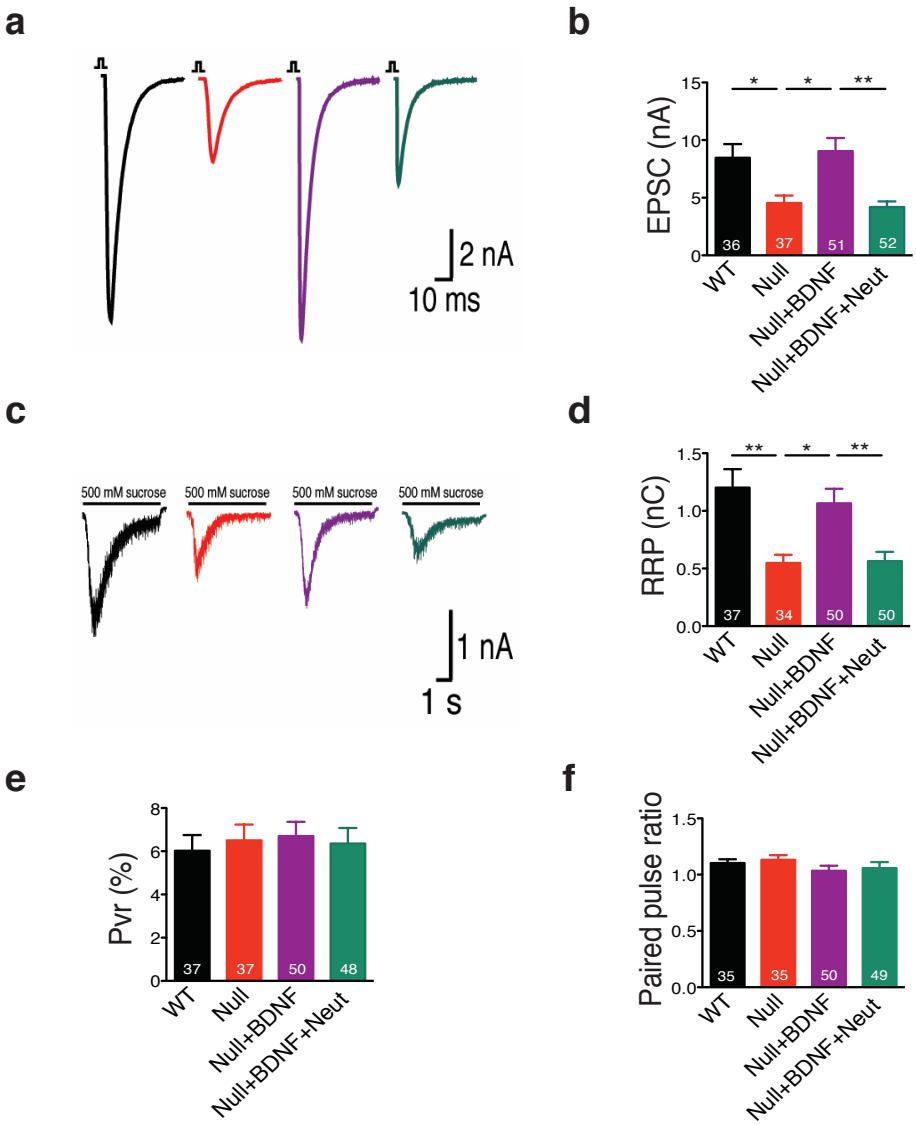

Figure 15. BDNF neutralization fails to rescue synaptic output in *Mecp2*$^{Null/y}$ neurons.

(a) Representative traces of evoked EPSCs recorded from autapses under the following conditions: WT, Null, Null + BDNF, Null + BDNF + neutralization. (b) Bar graph shows mean evoked EPSC amplitude. (c) Representative traces of average current response to 5 s application of 500 mM sucrose. Experimental groups same as (a). (d-f) Bar graphs show mean RRP size (d), P_{vr} (e) and 25 ms ISI – PPR (f).
Number of neurons (n) shown in the bars for all graphs. Data shown as mean ± SEM.
*$p < 0.05$; **$p < 0.01$; ns: not significant.

3.5. Lentivirus-mediated NGF overexpression in *Mecp2*$^{Null/y}$ neurons failed to rescue synaptic function

As an additional control experiment, we tested if overexpression of another neurotrophin - nerve growth factor (NGF) - yielded similar rescue of synaptic phenotype (Figure 16).

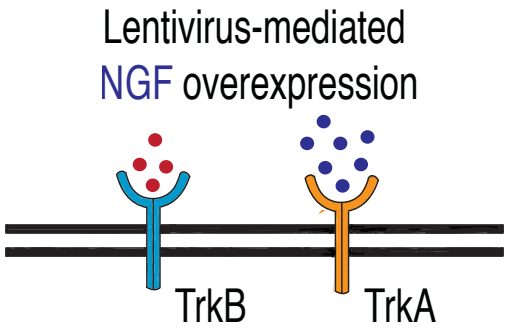

Figure 16. Experimental scheme of lentivirus-mediated NGF overexpression in *Mecp2*$^{Null/y}$ neurons, showing neuronal membrane (black), BDNF (red), TrkB receptor (blue), NGF (dark blue) and TrkA receptor (yellow).

We found that lentivirus-mediated NGF overexpression in either WT or *Mecp2*$^{Null/y}$ neurons failed to restore normal synaptic transmission including evoked EPSC amplitude and RRP size (Figure 17a and 17b). PPR and P_{vr} values were unaffected upon NGF overexpression (Figure 17c and 17d).

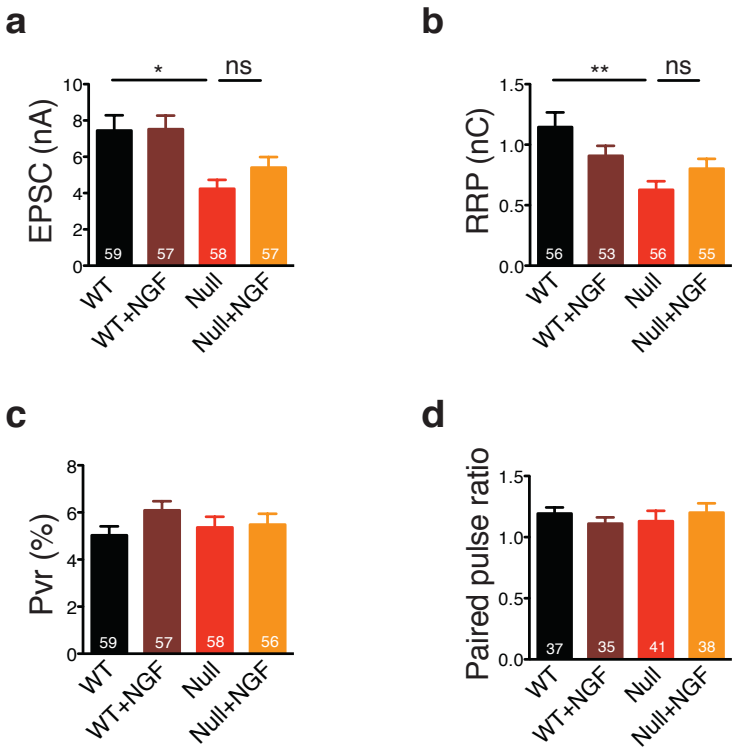

Figure 17. NGF overexpression in *Mecp2*$^{Null/y}$ neurons does not rescue glutamatergic synaptic output.
(a-d) Bar graphs show mean evoked EPSC amplitude (a), RRP size (b), P_{vr} (c) and 25 ms ISI – PPR (d).
Number of neurons (n) shown in the bars for all graphs. Data shown as mean ± SEM.
*p < 0.05; **p < 0.01; ns: not significant.

This observation further emphasized the specificity of BDNF-mediated phenotype rescue and affirmed the role of BDNF-TrkB signaling in regulating synapse formation in RTT-like glutamatergic neurons.

3.6. Exogenous BDNF application in *Mecp2*$^{Null/y}$ neurons rescues physiological and morphological phenotypes

Alternatively, we carried out an experiment involving long-term, exogenous application of BDNF to WT and *Mecp2*$^{Null/y}$ autaptic neurons to verify if we could bypass MeCP2 deficiency and obtain phenotype rescue similar to that of BDNF overexpression (Figure 18). Neurons were treated with 50 ng/ml of recombinant human BDNF at DIV 2 and replenished every 2-3 days until DIV 14 when they were either taken for electrophysiological measurements or fixed for morphology analysis.

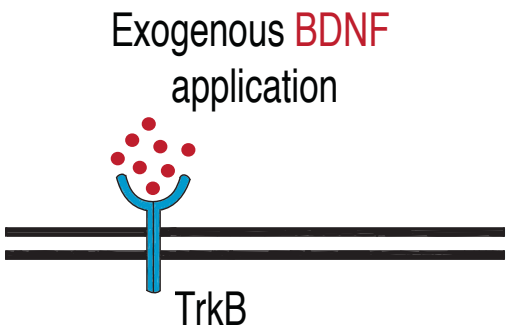

Figure 18. Experimental scheme depicting exogenous application of BDNF in *Mecp2*$^{Null/y}$ neurons, showing neuronal membrane (black), BDNF (red) and TrkB receptor (blue).

Exogenous BDNF application in *Mecp2*$^{Null/y}$ neurons normalized both physiological as well as morphological phenotypes. In particular, evoked EPSC amplitude and RRP size (Figure 19a and 19b), as well as dendrite length, glutamatergic synapse number and soma size (Figure 19c-e) were rescued back to WT levels. Phenotype specificity to BDNF-TrkB signaling was verified by ANA-12 application to *Mecp2*$^{Null/y}$ neurons treated with exogenous BDNF. We found that evoked EPSC amplitude and RRP size were decreased by 44% and 66% respectively upon ANA-12 application (Figure 19a and 19b). Similarly, ANA-12 application reverted synapse number, dendrite length and soma size back to Null levels, displaying a 39%, 47% and 28% decrease, respectively (Figure 19c and 19d). No significant changes were seen either in PPR or P_{vr} measurements upon BDNF application (Figure 20a and 20b).

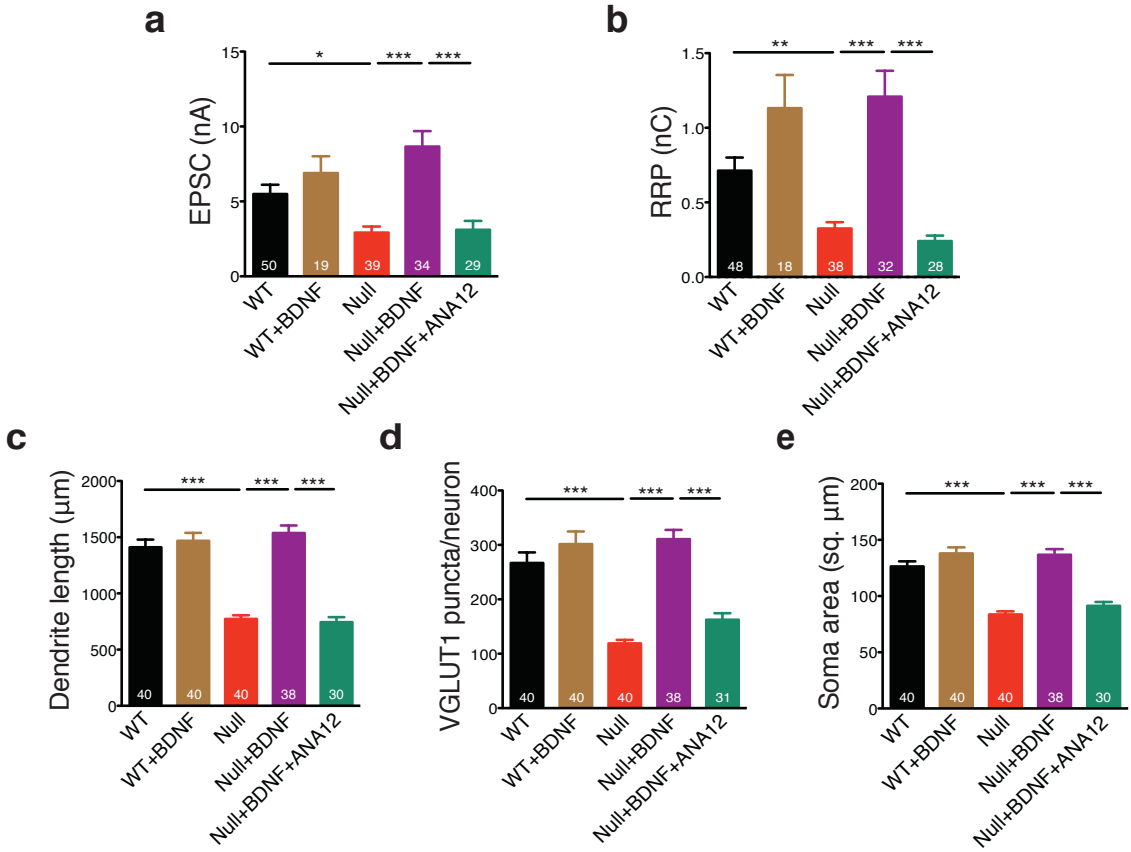

Figure 19. Exogenous application of BDNF restores physiological and morphological phenotypes, reaffirming specificity of BDNF-TrkB interaction in *Mecp2*$^{Null/y}$ glutamatergic neurons.
(a-e) Bar graphs show mean evoked EPSC amplitude (a), RRP size (b), dendrite length (c), glutamatergic synapse number (d) and neuronal soma area (e).
Number of neurons (n) shown in the bars for all graphs. Data shown as mean ± SEM.
*p < 0.05; **P < 0.01; ***p < 0.001; ns: not significant.

These findings proved that *Mecp2*$^{Null/y}$ neurons were deficient in BDNF synthesis and revealed impaired BDNF-TrkB signaling which was fully restored upon exogenous application of BDNF.

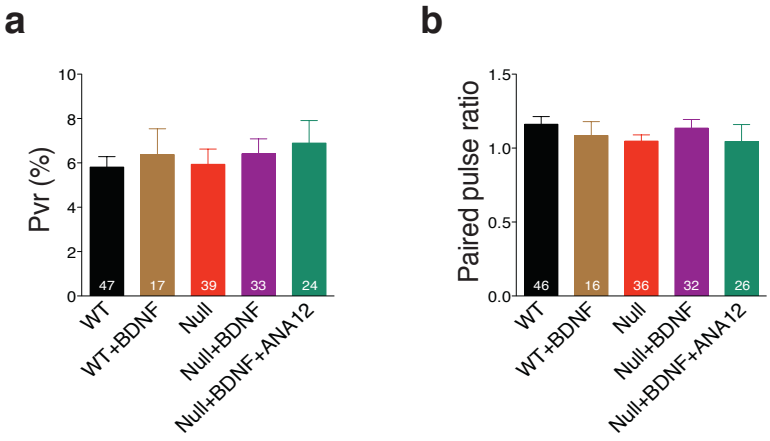

Figure 20. Exogenous application of BDNF does not alter release efficiency or short-term plasticity in *Mecp2*$^{Null/y}$ hippocampal neurons.
(a,b) Bar graphs show mean P_{vr} (a) and 25 ms ISI – PPR (b).
Number of neurons (n) shown in the bars for all graphs. Data shown as mean ± SEM.

3.7. An active BDNF-TrkB signaling pathway regulates glutamatergic synapse number in a cell-autonomous manner in an *in vitro* RTT model

We have shown that BDNF synthesis deficiency contributes towards the loss-of-function phenotype in *Mecp2*$^{Null/y}$ glutamatergic neurons. Further, restoring normal levels of BDNF via lentivirus-mediated overexpression (Figure 9-12) or exogenous application (Figure 19 and 20) facilitated rescue of morphological and physiological phenotypes thereby normalizing glutamatergic synapse formation to WT conditions.

Since MeCP2 is an X-linked gene, *Mecp2*$^{+/-}$ mice show mosaic expression of WT and mutant MeCP2 due to random X-chromosome inactivation, the main consequences being a much less severe phenotype and delay in RTT-like phenotype as compared to male hemizygous mice (*Mecp2*$^{Null/y}$). Hence, most studies are carried out in *Mecp2*$^{Null/y}$ mice although *Mecp2*$^{+/-}$ is the closest mouse model mimicking RTT. Additionally, WT neurons in RTT patients may not be able to rescue synapse number loss in neighboring MeCP2-deficient neurons despite mosaic expression of WT and mutant MeCP2. To incorporate this RTT-like condition in our culture system, we designed an *in vitro* model and examined if BDNF-TrkB signaling has an autocrine/paracrine preference for regulation of synapse formation in MeCP2-deficient neurons.

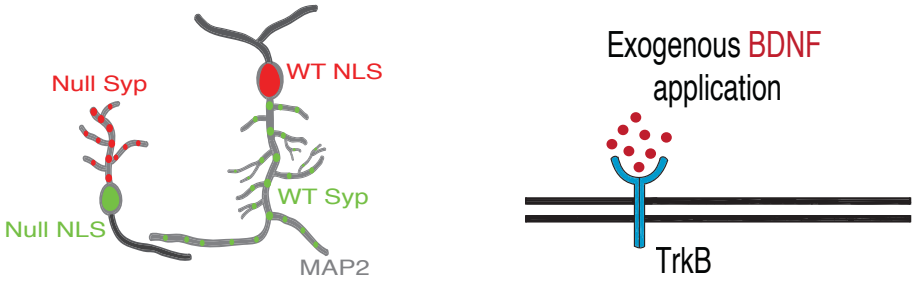

Figure 21. Left panel: Neuronal pair depicting lentivirus-mediated labeling of nucleus (NLS) and synapses of WT (NLS: red, Synaptophysin: green) and *Mecp2*$^{Null/y}$ neurons (NLS: green, Synaptophysin: red), co-stained for MAP2 to identify synapses localized on dendrites. **Right panel:** Experimental scheme of lentivirus-mediated BDNF overexpression in WT or *Mecp2*$^{Null/y}$ neurons, showing neuronal membrane (black), BDNF (red) and TrkB receptor (blue).

We co-cultured WT and *Mecp2*$^{Null/y}$ hippocampal neurons in a culture dish and analyzed glutamatergic synapse density (Figure 21-left panel). We took advantage of the lentiviral system and labeled neurons of either genotype with specific fluorescent markers to identify neuronal genotype as well as origin of synapses. We specifically examined glutamatergic synapses by double-labeling with VGLUT1 and MAP2 and analyzed VGLUT1+ and MAP2+ colocalizing Synaptophysin puncta across defined dendritic regions of interest (Figure 22a-left panel). We found that MeCP2-deficient glutamatergic neurons showed 34% decrease in synapse density when compared to co-cultured WT neurons (Figure 22b). This showed that excitatory synapse formation was disrupted in *Mecp2*$^{Null/y}$ hippocampal neurons in a RTT-like mosaic model similar to data obtained from autaptic neurons.

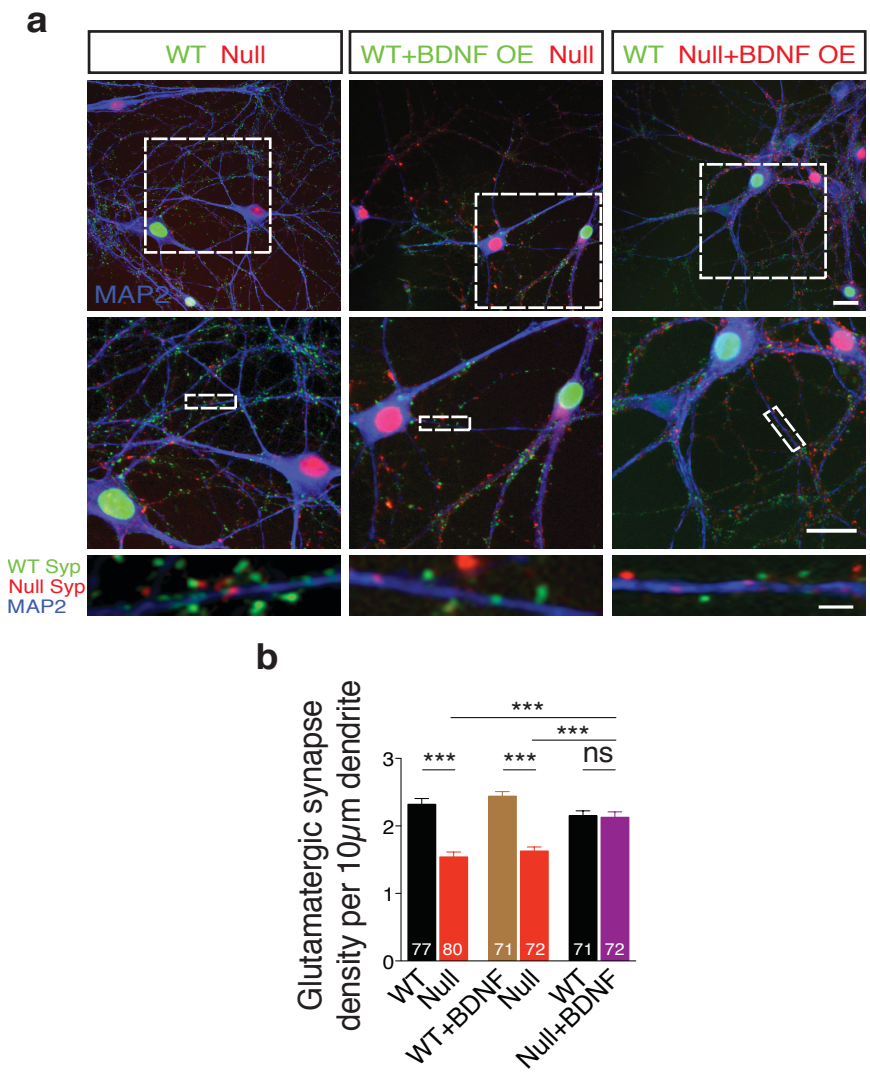

Figure 22. TrkB activation in *Mecp2*$^{Null/y}$ neurons in an *in vitro* RTT model normalizes glutamatergic synapse number in a cell-autonomous and autocrine manner.

(a) Representative images of co-cultured WT and *Mecp2*$^{Null/y}$ neurons labeled with MAP2 under the following conditions (from left to right): WT/Null; WT+BDNF/Null and WT/Null+BDNF. Bottom panel shows WT (green) and Null (red) Synaptophysin+ synapses localized on a single dendrite. Scale bars on top and middle panel represents 20 μm. Scale bar on bottom panel represents 3 μm. (b) Bar graph shows glutamatergic synapse density for all co-cultured groups.

Number of neurons (n) shown in the bars for all graphs. Data shown as mean ± SEM. ***$p < 0.001$; ns: not significant.

We then probed the effect of BDNF overexpression on WT and MeCP2-deficient neurons by pre-incubating them with specific lentiviral constructs, expressing both BDNF as well as Synaptophysin-GFP (WT) or Synaptophysin-mKate (*Mecp2*$^{Null/y}$) tagged to NLS-RFP or GFP respectively, using P2A and T2A self-cleaving peptides, respectively (Figure 21-right panel) (See Methods for details). These neurons were then co-cultured and glutamatergic synapse density was estimated as described before (Figure 22a-middle and right panel). Overexpressing BDNF in WT neurons did not have any effect on glutamatergic synapse density of either WT or proximate MeCP2-lacking cells with *Mecp2*$^{Null/y}$ glutamatergic synapses still reduced by 35% (Figure 22b). However, BDNF overexpressing *Mecp2*$^{Null/y}$ neurons displayed a significant restoration of synapse number up to 99% of WT levels, confirming that only increased BDNF levels in *Mecp2*$^{Null/y}$ neurons enabled rescue of glutamatergic synapse formation in a RTT-like culture system (Figure 22b).

These findings demonstrated a cell-autonomous and autocrine role for BDNF-TrkB activity in driving glutamatergic synapse formation in WT and *Mecp2*$^{Null/y}$ hippocampal neurons. Furthermore, these data highlight a highly focal effect for BDNF function in regulating excitatory synapses.

3.8. Exogenous application of a TrkB agonist restores glutamatergic synapse number in *Mecp2*$^{Null/y}$ neurons in a mixed co-culture system

So far, we found that WT neurons could not facilitate synapse number rescue in neighboring co-cultured MeCP2-deficient neurons elucidating the cell-autonomous role of MeCP2. Additionally, we also observed that lentivirus-mediated BDNF overexpression specifically in *Mecp2*$^{Null/y}$ neurons enabled phenotypic rescue which illustrated the requirement for an autocrine and localized BDNF-TrkB signaling pathway in these neurons (Figure 22b). We next examined the possibility of bypassing BDNF deficiency and exogenously

activating TrkB receptors in a RTT-like model. For this purpose, we applied a TrkB agonist - 7,8-dihydroxyflavone (7,8-DHF) - to WT and *Mecp2*$^{Null/y}$ co-cultured neurons, that binds to its extracellular domain and activates TrkB-mediated downstream signaling (Figure 23a).

Application of 500 nM 7,8-DHF at DIV 6, 9 and 12 normalized glutamatergic synapse number across all experimental conditions. *Mecp2*$^{Null/y}$ synapses were restored back up to 94% and 97% of WT synapse number when co-cultured with WT neurons and WT neurons overexpressing BDNF, respectively (Figure 23b). As seen before, 7,8-DHF application did not influence glutamatergic synapse number in WT or *Mecp2*$^{Null/y}$ neurons overexpressing BDNF, demonstrating that BDNF-TrkB signaling was sufficiently active in these neurons (Figure 23b).

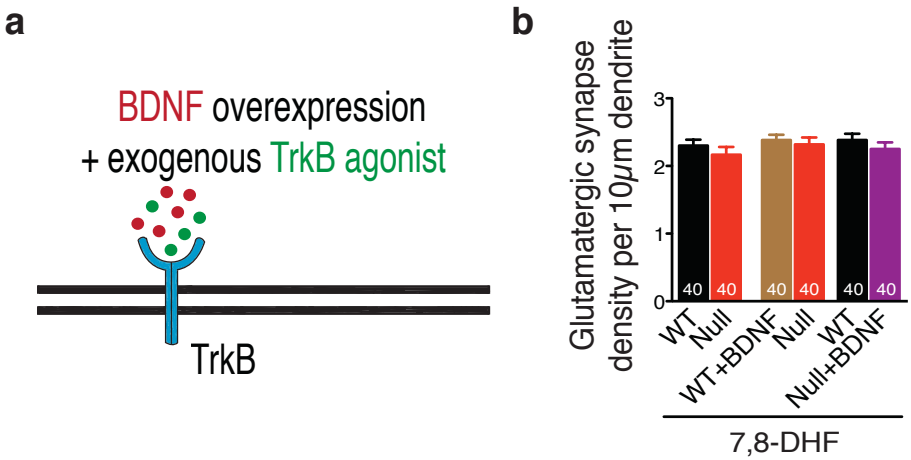

Figure 23. Application of a TrkB agonist restores glutamatergic synapse number in *Mecp2*$^{Null/y}$ neurons in a RTT-like *in vitro* model.
(a) Experimental scheme of lentivirus-mediated BDNF overexpression and exogenous application of TrkB agonist in WT or *Mecp2*$^{Null/y}$ neurons, showing neuronal membrane (black), BDNF (red), TrkB receptor (blue) and TrkB agonist (green). (b) Bar graph shows glutamatergic synapse density for all co-cultured groups upon application of TrkB agonist, 7,8-DHF.
Number of neurons (n) shown in the bars for all graphs. Data shown as mean ± SEM.

These findings confirmed that application of the TrkB agonist was able to bypass BDNF synthesis deficiency, exogenously activate TrkB and enhance synapse formation in *Mecp2*$^{Null/y}$ glutamatergic neurons. This further explains an important mechanistic role for BDNF wherein BDNF acts cell-autonomous and autocrine via TrkB receptor activation in a positive feed-forward fashion to regulate normal growth and synapse formation of MeCP2-deficient neurons.

3.9. BDNF acts as a presynaptic rate-limiting factor in regulating glutamatergic synapse formation in MeCP2-deficient neurons

We now asked if BDNF synthesis deficiency in *Mecp2*$^{Null/y}$ glutamatergic neurons influenced regulation of synapse number by affecting pre- or postsynaptic factors. We examined this question by repeating the previous experiment under defined conditions of analysis. Initially, we identified proximal dendrites of WT and *Mecp2*$^{Null/y}$ neurons to distinguish post- from presynaptic neurons (Figure 24). We then measured WT and *Mecp2*$^{Null/y}$ glutamatergic synapse densities as described above, formed on to WT and *Mecp2*$^{Null/y}$ postsynaptic neurons with or without BDNF overexpression. We hypothesized that in case of a predominantly presynaptic mechanism, *Mecp2*$^{Null/y}$ glutamatergic synapses would remain unchanged irrespective of the genotype of the postsynaptic neuron.

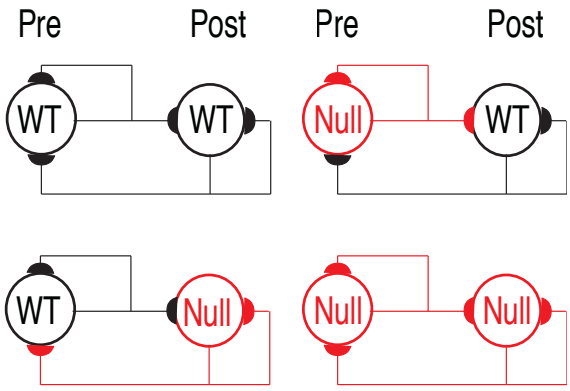

Figure 24. Example two-neuron scheme illustrating pre- and postsynaptic neurons (WT or *Mecp2*$^{Null/y}$) forming synapses onto itself or onto the partner neuron, in a mixed WT/*Mecp2*$^{Null/y}$ co-culture system.

Indeed, we observed that *Mecp2*$^{Null/y}$ glutamatergic synapse density formed on to WT and *Mecp2*$^{Null/y}$ postsynaptic neurons was 56% (Figure 25-left panel) and 45% (Figure 25-middle panel) decreased respectively. On the other hand, *Mecp2*$^{Null/y}$ neurons overexpressing BDNF showed increased number of glutamatergic synapses on to WT and *Mecp2*$^{Null/y}$ postsynaptic neurons with restored levels up to 87% and 86% of that of WT (Figure 25-right panel).

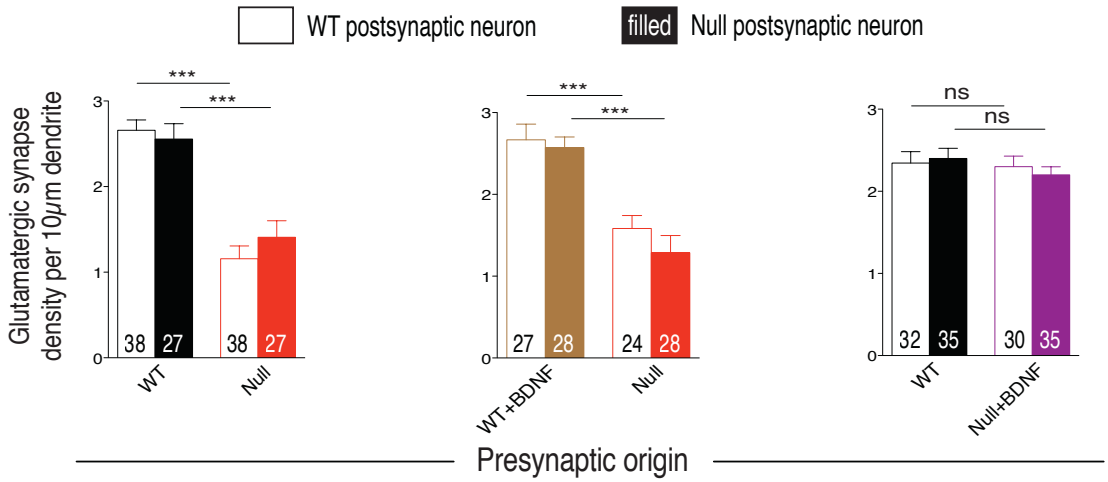

Figure 25. Cell-autonomous BDNF-TrkB signaling regulates glutamatergic synapse number by functioning as a presynaptic rate-limiting factor.
Bar graphs show glutamatergic synapse density measured from a postsynaptic WT (clear bars) and *Mecp2*$^{Null/y}$ (filled bars) neuron for the following experimental groups: (from left to right) WT/*Mecp2*$^{Null/y}$; WT+BDNF/*Mecp2*$^{Null/y}$; WT/*Mecp2*$^{Null/y}$+BDNF. Number of neurons (n) shown in the bars for all graphs. Data shown as mean ± SEM. ***$p < 0.001$; ns: not significant.

These data suggest that overall glutamatergic synaptic output is affected by BDNF synthesis deficit without disrupting excitatory innervation.

3.10. BDNF is partially located on the cell surface as stable deposits upon stimulation in WT and *Mecp2*$^{Null/y}$ neurons

Several peptidergic hormones and secretory molecules including Wnt (Papkoff and Schryver, 1990), Semaphorin 3A and BDNF (de Wit et al., 2009) have been shown to remain membrane resident. Considering that BDNF acts as an autocrine factor and drives neuronal growth in a cell-autonomous fashion, we examined the fate of BDNF secretion in WT and *Mecp2*$^{Null/y}$ hippocampal neurons. We designed an assay to monitor BDNF exocytosis in hippocampal neurons using a construct expressing BDNF tagged with superecliptic pHluorin (SpH) (Kolarow et al., 2007). BDNF-SpH was expressed in primary hippocampal neurons and characterized using the pHluorin live-cell imaging assay (Figure 26). We found that 60 mM KCl-induced membrane depolarization of BDNF-SpH-expressing neurons resulted in an increase in fluorescence (ΔF) that resembled a punctate-pattern distribution representative of BDNF exocytosis (Figure 27a). Vesicle de-acidification with 50 mM NH_4Cl indicated an abrupt increase in fluorescence enabling visualization of all fluorescent puncta followed by a gradual decay characteristic of BDNF diffusion out of the vesicle into the extracellular medium (Figure 27a and 27b).

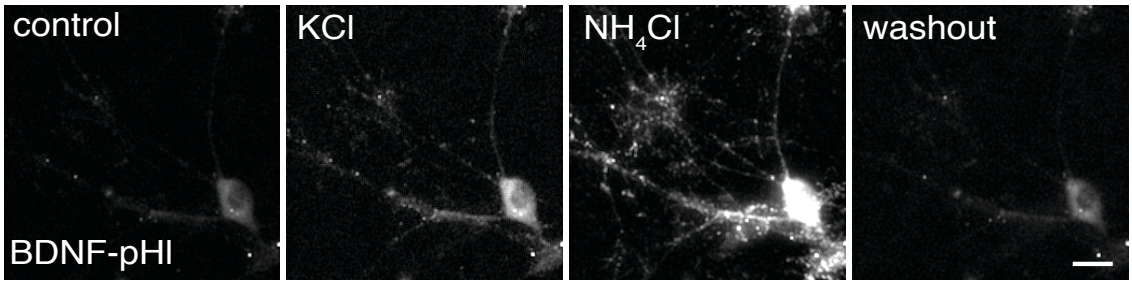

Figure 26. Representative images of a WT hippocampal neuron expressing BDNF-superecliptic pHluorin perfused with standard extracellular solution, 60 mM KCl, 50 mM NH_4Cl and washout with extracellular solution (left to right). Scale bar represents 10 μm.

We then studied individual fusion events in WT (Figure 27c) and *Mecp2*$^{Null/y}$ (Figure 27d) hippocampal neurons and observed that upon KCl-induced stimulation, both genotypes revealed several fluorescent puncta with varying degrees of decrease in fluorescence indicative of fusion events some of which decayed abruptly while many others decayed slowly or remained persistent. Majority of fusion events in WT and *Mecp2*$^{Null/y}$ neurons were predominantly transient and decayed immediately back to baseline level while a fraction remained persistent (slow/no dimming in fluorescence). Quantification of all events showed that activity-induced BDNF secretion was unaffected in *Mecp2*$^{Null/y}$ neurons (WT: 34%, n=1464 events; Null: 31%, n=895 events) (Figure 27e).

To investigate persistent events, neurons were subjected to MES-buffered acidic solution, pH 5.5, to acidify the exterior so as to estimate the proportion of BDNF vesicle cargo present on the membrane surface (Figure 27a). Acid perfusion following KCl-induced stimulation caused an instant decrease in fluorescence and acid quenched BDNF fraction was normalized to corresponding peak NH_4Cl response. Analysis showed that WT and *Mecp2*$^{Null/y}$ neurons showed a 26% and 28% decrease in fluorescence respectively (WT: n=1480 events, Null: n=900 events) (Figure 27f), which reflects the non-internalized pool of BDNF vesicles that are either found on the neuronal surface or easily accessible from the extracellular space around the cell membrane. This indicates that both WT and *Mecp2*$^{Null/y}$ neurons accommodate partial fraction of BDNF as neuronal membrane-resident deposits acting as a reservoir for activation of endogenous TrkB receptors.

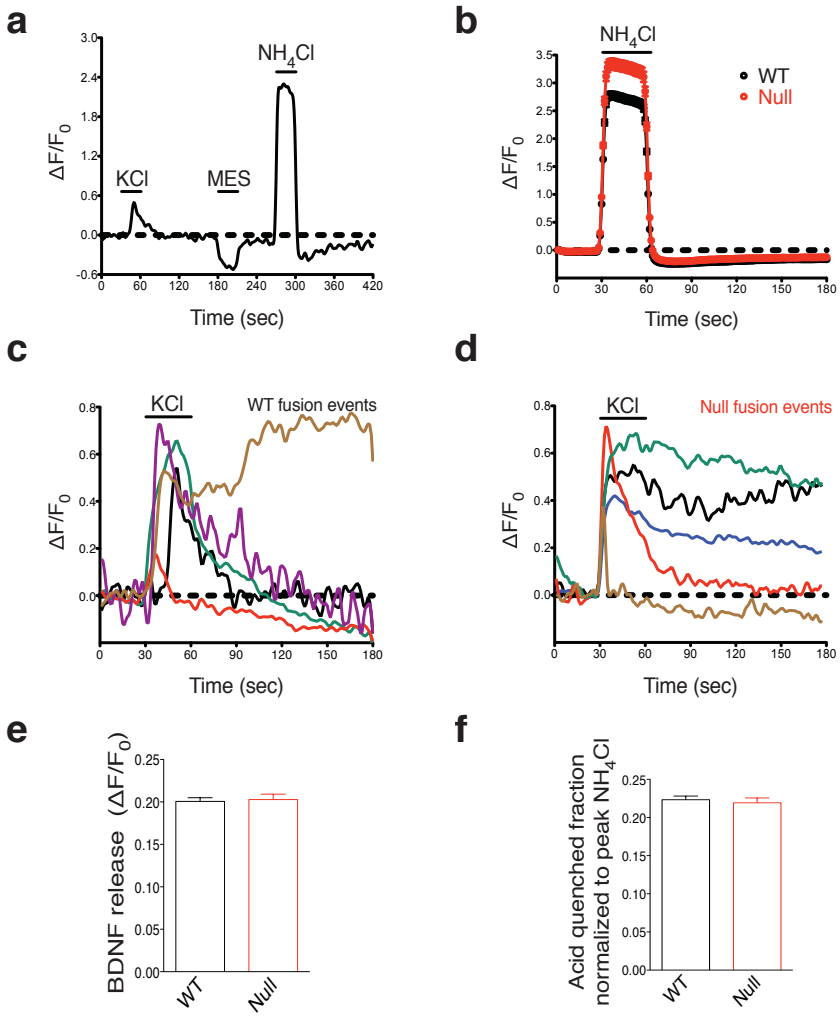

Figure 27. WT and *Mecp2*$^{Null/y}$ hippocampal neurons reveal transient and persistent fusion events upon stimulation, show equivalent activity-dependent BDNF secretion and membrane-resident BDNF-SpH fraction.

(a) BDNF fluorescence ($\Delta F/F_0$) over time reflecting fusion events upon application of KCl, MES and NH_4Cl solutions. Black line indicates duration of KCl, MES and NH_4Cl application. (b) Mean BDNF fluorescence ($\Delta F/F_0$) after NH_4Cl application (WT, 1521 events, *Mecp2*$^{Null/y}$, 948 events). (c,d) Representative traces of BDNF fluorescence ($\Delta F/F_0$) indicating transient and persistent fusion events upon KCl-induced membrane depolarization in WT (c) and *Mecp2*$^{Null/y}$ neurons (d). (e,f) Bar graphs show activity-dependent BDNF release (e) and BDNF-SpH surface fraction upon acid wash (MES, pH 5.5) (f) in WT and *Mecp2*$^{Null/y}$ neurons.

Error bars represent ± SEM. Data shown as mean ± SEM.

These results are in congruence with previous findings and explain why WT neurons are unable to facilitate rescue of proximal 'Null' synapses in a RTT-like model. Secreted BDNF signals are partially retained at the cell surface hence mainly triggering activation of its own TrkB receptors (autocrine) as opposed to additionally binding and activating adjacent TrkB receptors (paracrine).

3.11. Hippocampal CA1 MeCP2-deficient neurons of female heterozygous mice have smaller nuclei as compared to wildtype neurons

We have seen so far that BDNF functions in an autocrine and cell-autonomous fashion in regulating neuronal growth and synaptic function in a MeCP2-dependent manner. This could imply that in female heterozygous mice with mosaic expression patterns of WT and mutant MeCP2, deficit of BDNF synthesis and release may partially be responsible for a persistent growth phenotype in neurons expressing mutant MeCP2 *in vivo*. Neuronal growth and development was affected in neurons lacking MeCP2 in single cells as well as in other culture systems. In particular, nuclei size has been known to be consistently smaller in MeCP2-deficient neurons (Chen et al., 2001; Rietveld et al., 2015) and rescued back up to WT levels upon administration of the TrkB agonist 7,8-DHF to *Mecp2*$^{Null/y}$ mice (Johnson et al., 2012). Hence, we examined the nucleus size of MeCP2+ and MeCP- neurons in the hippocampal CA1 of 2- and 8-week old *Mecp2*$^{+/-}$ female mice (Figure 28a).

We performed this experiment by labeling the hippocampal CA1 for MeCP2 and DAPI to investigate if neurons exhibit a persistent growth phenotype in a MeCP2-dependent manner. We quantified nucleus size of MeCP2+ and MeCP2- neurons from mice of both ages. Intriguingly, we found that MeCP2-deficient neuronal nuclei were 18% and 21% smaller than MeCP2+ neurons in 2- (Figure 28b) and 8-week old (Figure 28c) *Mecp2*$^{+/-}$ mice

respectively. Together with the previous *in vitro* findings, this *in vivo* data strongly suggest a cell-autonomous role for BDNF secretion in MeCP2 mutant mice and pave way for future studies investigating the correlation of MeCP2 loss-of-function and BDNF cell-autonomy.

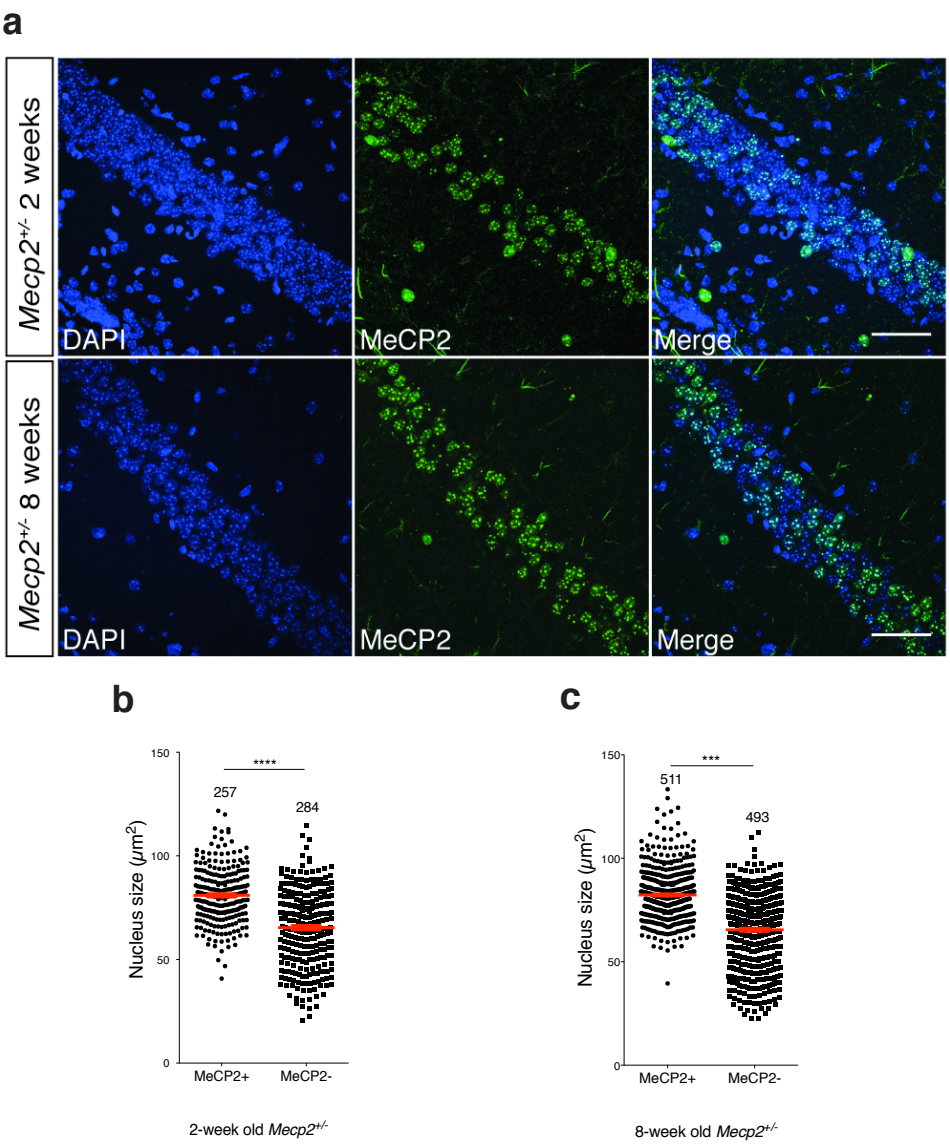

Figure 28. Hippocampal CA1 neurons lacking MeCP2 have smaller neuronal nuclei in *Mecp2*$^{+/-}$ mice.

(a) Representative images of hippocampal CA1 from *Mecp2*$^{+/-}$ mice labeled for DAPI (blue) and MeCP2 (green) at 2- (top) and 8-weeks of age (bottom). Scale bar represents 50 μm. (b,c) Scatter plots show mean nuclei size of MeCP2+ and MeCP2- neurons at 2- (b) and 8-weeks of age (c).

Number of neurons (n) shown in the bars for all graphs. Data shown as mean ± SEM. ***$p < 0.001$; ****$p < 0.0001$.

Chapter 4: Discussion

4.1. General summary of findings

In this study, we have investigated the role of BDNF - a secreted molecule as well as a transcriptional target gene of MeCP2 - in regulating neuronal growth and differentiation and synaptic function of MeCP2 mutant glutamatergic hippocampal neurons. Previous studies have reported a MeCP2-dependent phenotype wherein glutamatergic synapse formation as well as dendritic complexity and arborization were significantly affected with loss of MeCP2 (Belichenko et al., 2009; Chao et al., 2007; Jentarra et al., 2010; Larimore et al., 2009; Zhou et al., 2006). However, underlying putative mechanisms are poorly understood.

First, we observed that MeCP2-deficient neurons displayed reduced axonal and dendritic outgrowths as well as smaller soma. By contrast, neurons expressing twice the levels of WT MeCP2 did not show any morphological abnormalities. Hence, we attempted to understand causal mechanisms underlying the loss-of-function phenotype associated with loss of MeCP2. Intriguingly, we found an essential role for BDNF.

Second, we report a complete rescue of synaptic output and neuronal morphology in MeCP2-deficient glutamatergic neurons upon lentivirus-mediated overexpression as well as exogenous application of BDNF. This highlights a major deficit in BDNF synthesis in *Mecp2*$^{Null/y}$ neurons.

Third, we demonstrate impaired BDNF-TrkB signaling in these neurons by application of the TrkB antagonist ANA-12 to WT and *Mecp2*$^{Null/y}$ glutamatergic neurons. Interestingly, chronic block of TrkB receptors by ANA-12 application converts WT neurons to a MeCP2-deficient state by impairing both physiological and morphological phenotypes, further illustrating complete suppression of the canonical BDNF-TrkB signaling pathway in *Mecp2*$^{Null/y}$ neurons.

Fourth, we verify the specificity of BDNF overexpression experiments by neutralizing BDNF that reverted synaptic output to *Mecp2*$^{Null/y}$ levels and NGF overexpression that failed to restore synapse function.

Fifth, we demonstrate that the BDNF-mediated growth pathway is strictly cell-autonomous from two important findings: (i) In a mixed co-culture system mimicking RTT *in vitro*, proximate WT neurons failed to restore normal synapse numbers in glutamatergic *Mecp2*$^{Null/y}$ neurons. (ii) In *Mecp2*$^{+/-}$ mice, hippocampal CA1 neurons lacking MeCP2 had smaller nuclei at 2- and 8-weeks of age demonstrating a persistent growth phenotype in mutant neurons *in vivo*. This was particularly elucidative given that BDNF mRNA levels were reduced in postmortem RTT brain samples (Abuhatzira et al., 2007; Deng et al., 2007) and BDNF protein levels were reduced in *Mecp2*$^{+/-}$ mice (Wang et al., 2006).

Sixth, we show that application of a TrkB agonist - 7,8-DHF - normalized glutamatergic synapse densities in neurons lacking MeCP2 indicating that exogenous activation of TrkB was able to bypass BDNF synthesis deficit and enhance BDNF-TrkB signaling in MeCP2 mutant neurons in a RTT model.

Seventh, we also observed presence of membrane-resident BDNF deposits in WT and *Mecp2*$^{Null/y}$ neurons without affecting activity-dependent BDNF secretion which further strengthens our hypothesis of a constitutive BDNF feed-forward signaling pathway for normal growth and differentiation and synapse formation in glutamatergic neurons. However, this crucial positive feed-forward mechanism remains impaired in MeCP2-deficient neurons.

Finally, we show that the impaired BDNF signaling pathway functions predominantly via impairment of presynaptic factors, since glutamatergic synapse densities remained independent of the genotype of the postsynaptic neuron.

4.2. BDNF-mediated phenotypic rescue in MeCP2 mutant mice

Several previous studies have reported manipulation of MeCP2 levels since reactivation of the *MECP2* gene has shown rescue of the loss-of-function phenotype associated with MeCP2 mutant RTT models (Chang et al., 2006; Chao et al., 2007; Guy et al., 2007; Kline et al., 2010; Larimore et al., 2009; McGraw et al., 2011; Nguyen et al., 2012). Besides MeCP2, manipulating protein levels of downstream target genes transcriptionally regulated by MeCP2 has resulted in phenotypic rescue at a cellular, circuit and behavioral level. In our autaptic as well as mixed co-culture system, we convincingly demonstrated that all morphological and physiological deficits observed could be linked to simply a deficiency of BDNF synthesis and release. This finding renders MeCP2-BDNF interaction extremely significant given that MeCP2 is known to regulate transcription of a wide range of target genes.

Along these lines, endogenous MeCP2 knockdown reduced dendritic length in E18 hippocampal neurons, which was fully rescued upon BDNF overexpression (Larimore et al., 2009). This is in agreement with our rescue data from single cells and mixed culture system. In congruence, exogenous application of BDNF reverted the amplitude of spontaneous miniature EPSCs and evoked EPSCs in nTS neurons, which was originally increased due to reduced levels of BDNF in the brainstem of *Mecp2*^{Null} mice (Kline et al., 2010). This rescue is comparable to the synaptic phenotype rescue seen in glutamatergic *Mecp2*$^{Null/y}$ neurons via increased levels of BDNF. This further emphasized the specificity of effects of BDNF differential expression across various brain regions.

4.3. Amelioration of Rett phenotypes by other therapeutic approaches

Much attention has been featured towards manipulating TrkB activation in MeCP2 mutant mouse models using small molecules that could potentially be substituted as TrkB agonists and activate sufficient TrkB signaling (Jang et al., 2010; Massa et al., 2010) in order to normalize synaptic, cellular and behavioral phenotypes in MeCP2-deficient neurons. This was based on earlier studies hypothesizing that BDNF was a secretory molecule with poor blood-brain barrier penetration characteristics (Poduslo and Curran, 1996) and hence unsuitable for therapeutic purposes.

7,8-DHF administration to MeCP2 mutant mice delayed body weight loss, increased size of CA1 neuronal nuclei and partially restored normal breathing patterns (Johnson et al., 2012). LM22A-4 normalized TrkB phosphorylation in the medulla and pons of heterozygous female MeCP2 mutant mice upon treatment for 4 weeks (Schmid et al., 2012), rescued hyperexcitability phenotype in the nTS of *Mecp2*^{Null} mice, and eliminated spontaneous apneas *in vivo* in *Mecp2*^{Null} and heterozygous mice upon acute treatment (Kron et al., 2014). In addition to molecules that activate TrkB, studies reveal other candidates including CX546 (Ogier et al., 2007), environmental enrichment (Kondo et al., 2008; Lonetti et al., 2010), insulin-like growth factor-1 (Tropea et al., 2009), cysteamine (Roux et al., 2012) and fingolimod (Deogracias et al., 2012) that improve various aspects during the course of RTT.

In the mixed co-culture model that we designed, we plated WT and *Mecp2*$^{Null/y}$ neurons together so as to create a RTT-like mosaic expression system. 7,8-DHF application to these co-cultured neurons demonstrated the ability of a TrkB agonist to reactivate TrkB signaling in *Mecp2*$^{Null/y}$ neurons up to WT levels. It also highlighted the autocrine and cell-autonomous function of BDNF crucial for regulation of glutamatergic synapse formation in WT and

Mecp2$^{Null/y}$ hippocampal neurons. Additionally, it substantiated the requirement of a constitutive BDNF feed-forward signaling pathway which was impaired in *Mecp2*$^{Null/y}$ excitatory neurons.

One possibility for this impaired BDNF-TrkB activity could be differential surface expression of postsynaptic TrkB receptors. This essentially indicates inadequate availability of surface TrkB receptors for binding to BDNF. However, we observed complete rescue of synaptic output (evoked EPSC amplitude and RRP size) as well as morphological parameters (dendrite length, glutamatergic synapse number and soma size) upon BDNF overexpression and exogenous application of BDNF. This led us to eliminate the possibility of differential TrkB expression and specifically elucidated an upstream deficit in synthesis and release of BDNF in MeCP2-deficient glutamatergic neurons. What is yet to be understood and beyond the aim of this thesis is how 7,8-DHF functions *in vitro* and *in vivo* to ameliorate RTT symptoms and facilitate rescue of synaptic and morphological phenotypes.

4.4. Cell-type specific effects of BDNF function in Rett syndrome

One of the most striking effects of the MeCP2-BDNF interaction has been the differential impact of loss of MeCP2 on BDNF regulation. For instance, although BDNF levels has been found to be reduced in the hippocampus, cortex and the brainstem (Chang et al., 2006), decreased BDNF levels contribute via different mechanisms and result in distinct phenotypes (Chang et al., 2006; Chao et al., 2007; Wang et al., 2006). Wang et al. reported a significant reduction in absolute amounts of BDNF released in *Mecp2*$^{Null/y}$ nodose ganglion (NG) neurons (Wang et al., 2006). However, the authors also observed an increase in percentage of BDNF content available for constitutive release. This study illustrates the dependence of BDNF-mediated morphological and physiological phenotypes on cell type and brain region.

In our investigation, we found that glutamatergic synaptic output is restored in MeCP2-deficient hippocampal neurons when BDNF levels are increased via BDNF overexpression or exogenous BDNF application. We also verified a deficit in BDNF synthesis and release through BDNF neutralization experiments. Indirectly, this suggests decreased availability of constitutive BDNF for release. Alternatively, previous studies have also hypothesized on parallel pathways by which BDNF could be functioning. In particular, activity-dependent BDNF release from presynaptic mossy fibers onto CA3 pyramidal neurons of symptomatic MeCP2 mutant mice was found to be decreased (Li et al., 2012). This phenotype was mechanistically correlated to impaired TRPC3 signaling.

What is yet to be determined is how this impaired BDNF-TrkB signaling relates to other cell types in the brain. Glutamatergic neurons comprise 90% of all neurons in the central nervous system and form the major excitatory class of neurons in the brain. Alternatively, GABAergic neurons are the most important inhibitory neurons. Normal excitation - inhibition balance in circuitries is

extremely crucial for proper functioning of the CNS and abnormal E/I balance has been known to be a major causal contributing factor in several neurodevelopment disorders (Dani et al., 2005; Desai et al., 1999; Kleschevnikov et al., 2004). This has prompted several researchers to investigate the individual roles of MeCP2-deficient glutamatergic and GABAergic neurons in different RTT-like mouse models (Chao et al., 2010; Chao et al., 2007). These studies have enabled preliminary understanding of the interaction between excitatory and inhibitory neurons with regard to autism and other classic neurodevelopment disorders such as RTT (Sohal et al., 2009; Yizhar et al., 2011).

Intriguingly, MeCP2-deficient glutamatergic and GABAergic neurons show very distinct phenotypes. For example, *Mecp2*$^{Null/y}$ excitatory neurons show reduced evoked EPSC amplitudes and a smaller RRP size. Additionally, loss of MeCP2 reduced frequency of spontaneous excitatory events in hippocampal autaptic neurons (Chao et al., 2007). By contrast, loss of MeCP2 resulted in a decrease of GABA release which was evident from the reduced mIPSC amplitudes in autaptic GABAergic neurons as well as in cortical slices. Moreover, *MECP2* was found to bind to the promoter region of *GAD1* and *-2*, thus regulating production of GABA synthesizing enzymes. Interestingly, loss of MeCP2 in GABAergic neurons from mouse hippocampal slices led to an overall decrease in output function which was evident from the increased input - output function of evoked excitatory postsynaptic responses and a lower threshold for induction of long-term potentiation (LTP) (Chao et al., 2010). Reduced LTP was observed in *Mecp2*$^{Null/y}$ cortical slices (Asaka et al., 2006) while enhanced LTP was seen in *MECP2*^{Tg1} hippocampal slices (Collins et al., 2004). However, no changes in GABAergic synapse formation were seen unlike glutamatergic neurons although BDNF released from postsynaptic target neurons acts locally to modulate GABAergic synapse formation (Kohara et al., 2007). Hence, it would be interesting to study the role of BDNF signaling in inhibitory neurons not only to understand the impact of BDNF-TrkB activity on GABAergic neurons

but also to investigate its effect on overall excitation - inhibition balance in autism spectrum disorders.

4.5. Surface deposition of BDNF and other secretory molecules

Several peptidergic hormones and secretory molecules including BDNF (de Wit et al., 2009) and other neurotrophins (Blochl and Thoenen, 1996; Brigadski et al., 2005), Wnt (Cadigan et al., 1998; Papkoff and Schryver, 1990) and Semaphorin (Bouzioukh et al., 2006; De Wit et al., 2005; de Wit et al., 2009; Sahay et al., 2005) are known to remain membrane - resident after secretion. Specifically, BDNF is found to bind to the cell surface mainly due to its highly positive charge at physiological pH, and locally modulates developing synapses by spatially restricting BDNF action (Zhang and Poo, 2002).

Indeed in our culture system, we found that BDNF partially remains membrane - resident post secretion. This reaffirms that such stable membrane deposits partially contribute towards the cell-autonomous regulation of synapse formation in MeCP2-deficient glutamatergic hippocampal neurons at single-cell level by confining activity of BDNF-TrkB to its own neurites. Furthermore, our data suggest a deficit in constitutive BDNF release in *Mecp2*$^{Null/y}$ excitatory neurons that may be responsible for the observed synaptic phenotypes since activity-dependent regulated BDNF release was unaffected as shown by BDNF-SpH experiments.

4.6. Cell-autonomous regulation of glutamatergic synapse formation in MeCP2 mutant mice

The persistent growth phenotype demonstrating smaller nuclei in MeCP2-deficient neurons is a critical example of cell-autonomy of MeCP2-BDNF interaction (Figure 28). This clearly shows that neighboring neurons expressing sufficient amounts of MeCP2 are nonetheless unable to facilitate rescue of normal growth and function in proximate MeCP2 mutant neurons.

Past studies have demonstrated conflicting results when studying MeCP2 cell autonomy. For example, a study reported both cell-autonomous and non cell-autonomous effects wherein MeCP2 female GFP mice aged 6-7 months displayed significant decrease in the density of spines, and spine head area specifically in MeCP2-deficient dendrites when compared to MeCP2+ neurons. However, MeCP2 GFP male mice aged three months showed reduced spine density and thinner apical oblique dendrites and increased dendritic irregularities and long spines indicating non cell-autonomous effects of MeCP2 (Belichenko et al., 2009). In a similar study, transplanted MeCP2-deficient layer 2/3 pyramidal neurons exhibited reduction in dendritic complexity and were smaller than transplanted wildtype neurons independent of recipient environment, indicating that the phenotype of MeCP2-deficient pyramidal neurons largely resulted from cell-autonomous mechanisms with additional non cell-autonomous effects (Kishi and Macklis, 2010).

A third study investigated homeostatic synaptic scaling in rat visual cortical pyramidal neurons and found that acute RNAi knockdown of MeCP2 blocked synaptic scaling by decreasing excitatory synapse number without affecting basal mEPSC amplitude or AMPAR accumulation at spared synapses (Blackman et al., 2012). This demonstrated that MeCP2 acts cell-autonomously to maintain both excitatory synapse number and synaptic scaling. These data show examples of MeCP2 having a mixed cell-autonomous as well as non cell-autonomous role in synaptic function and growth of glutamatergic neurons. Our data showing reduced glutamatergic synapse densities in a mixed co-culture

system strongly indicate a cell-autonomous role for MeCP2 *per se*. Moreover, we demonstrate restored synapse number in glutamatergic *Mecp2*$^{Null/y}$ neurons only upon increasing levels of BDNF specifically in these neurons or upon external activation of TrkB receptors via TrkB agonist application. These findings strongly argue for autocrine BDNF activity and a cell-autonomous role for BDNF-TrkB signaling in glutamatergic synapse formation in MeCP2-deficient neurons. Furthermore, we observed a predominant role for the presynaptic site to be instructive of synapse formation since glutamatergic synapse number was influenced only by the presynaptic neuronal type and independent of genotype of the postsynaptic neuron.

However, further studies need to be carried out to understand this phenomena in detail directly addressing the following questions. (i) Does constitutive BDNF release contribute towards maintaining synapse formation in MeCP2-deficient glutamatergic neurons in a RTT model? (ii) Does the pre- or postsynaptic release of BDNF specifically determine normal neuronal growth and synaptic function in glutamatergic neurons lacking MeCP2? (iii) Do MeCP2 lacking neurons in female heterozygous *Mecp2*$^{+/-}$ mice particularly express reduced BDNF levels compared to neighboring WT MeCP2 neurons? These questions could help determine the locus of activity-dependent regulation of growth and excitatory synapses in RTT-like glutamatergic neurons.

4.7. Role of BDNF autocrine feed-forward signaling in glutamatergic synapse formation

It is important to understand the functional significance of this autocrine feed-forward mechanistic signaling mediated by BDNF. Neuronal activity has been known to play a major role in driving basic growth of neurons during development and BDNF is reported to be an essential factor in regulation of neuronal growth and synaptic function upon activity. *Mecp2*$^{Null/y}$ neurons exhibit reduced intrinsic activity across several cell types and brain regions (Chang et al., 2006; Chao et al., 2007; Dani et al., 2005; Tropea et al., 2009). This reduced activity may potentially disrupt activity-dependent neuronal growth and function.

The morphological and physiological deficits seen in MeCP2-deficient glutamatergic neurons could be rectified by simply supplying an additional source of BDNF or TrkB agonist both of which enhance TrkB receptor signaling and downstream intracellular signaling cascades. Specifically, application of 7,8-DHF to *Mecp2*$^{Null/y}$ neurons in a WT/*Mecp2*$^{Null/y}$ mixed co-culture system led to restoration of glutamatergic synapse densities strongly arguing for a highly localized and autocrine function for BDNF and cell-autonomous BDNF-TrkB signaling mechanism. This cell-autonomy further offers a plausible mechanism as to why phenotypes in MeCP2 mutant neurons in RTT females are independent of and not affected by MeCP2 mosaicism at a synaptic, circuit or behavioral level.

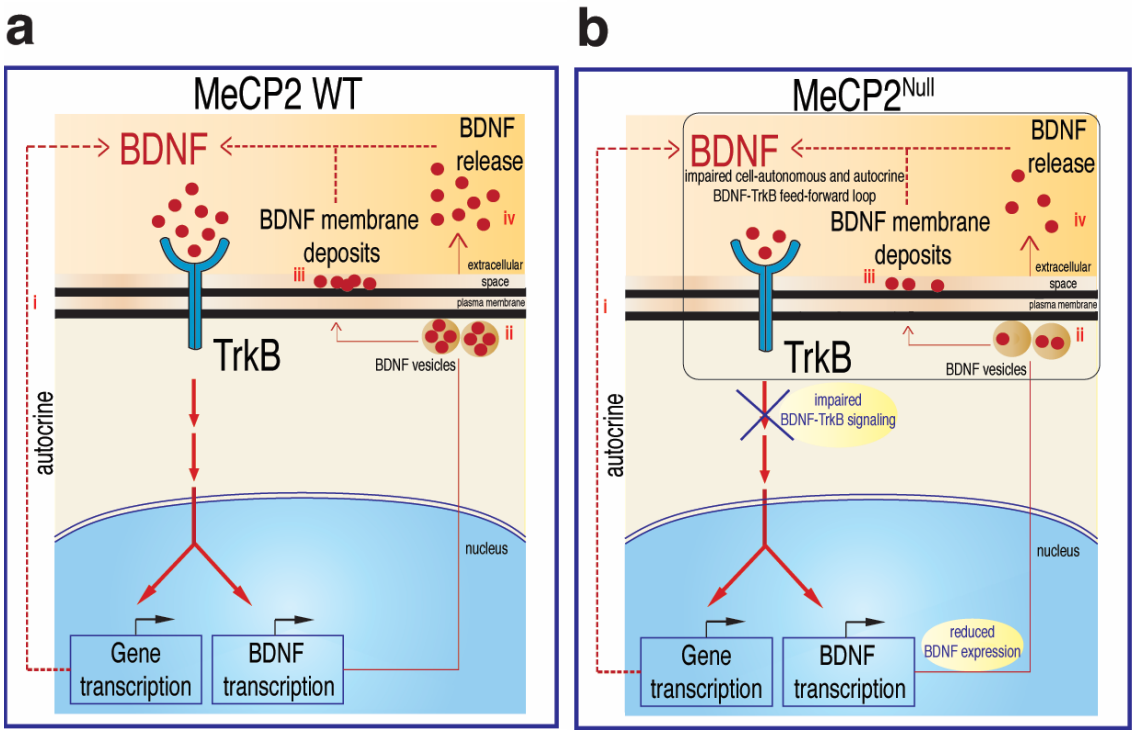

Figure 29. A diagram illustrating local BDNF-TrkB signaling in WT and *Mecp2*^{Null} hippocampal excitatory neurons. Activation of TrkB receptors by BDNF binding leads to transcriptional regulation of several downstream target genes including BDNF itself, triggering an autocrine loop (i). Deficiency of BDNF synthesis upon loss of MeCP2 results in reduced availability of BDNF secretory granules for release (ii). Partial membrane-resident BDNF deposits are found in both WT and *Mecp2*$^{Null/y}$ excitatory neurons (iii). Reduced BDNF synthesis leads to upstream deficit in BDNF synthesis and release resulting in impaired BDNF-TrkB signaling in *Mecp2*$^{Null/y}$ neurons (iv). This model highlights a highly localized and cell-autonomous BDNF-TrkB feed-forward signaling loop in WT neurons (a) which is disrupted in MeCP2-deficient neurons (b), causal of reduced glutamatergic synapse numbers in RTT models.

An open question is to investigate further if the predominant effect of impaired BDNF-TrkB signaling in *Mecp2*$^{Null/y}$ neurons originally arises from the pre- or postsynaptic site. Morphological analysis showed aberrations in both axonal as well as dendritic outgrowth upon loss of MeCP2. Additionally, mixed co-culture data indicated a presynaptic deficit wherein *Mecp2*$^{Null/y}$ glutamatergic synapses made onto the postsynaptic neuron was independent of genotype and was determined solely by the presynaptic site. This implies a major propagation defect in MeCP2 mutant neurons in a mosaic circuit wherein they receive synaptic input similar to WT neurons. However, these mutant neurons show reduced capacity to communicate output signal to a postsynaptic neuron which in turn reduced efficiency of innervation across specific brain regions and dampened synaptic output.

More generally, this study not only provides mechanistic insight into BDNF signaling in RTT-like MeCP2 mutant neurons but also substantiates the consequences of putative manipulation of BDNF-TrkB activity and its relevance in therapeutic strategies in ameliorating progression of the RTT disease.

Bibliography

Abuhatzira, L., Makedonski, K., Kaufman, Y., Razin, A., and Shemer, R. (2007). MeCP2 deficiency in the brain decreases BDNF levels by REST/CoREST-mediated repression and increases TRKB production. Epigenetics 2, 214-222.

Ajami, A., Hosseini, S.H., Taghipour, M., and Khalilian, A. (2014). Changes in serum levels of brain derived neurotrophic factor and nerve growth factor-beta in schizophrenic patients before and after treatment. Scand J Immunol 80, 36-42.

Amano, K., Nomura, Y., Segawa, M., and Yamakawa, K. (2000). Mutational analysis of the MECP2 gene in Japanese patients with Rett syndrome. J Hum Genet 45, 231-236.

Amir, R.E., Van den Veyver, I.B., Schultz, R., Malicki, D.M., Tran, C.Q., Dahle, E.J., Philippi, A., Timar, L., Percy, A.K., Motil, K.J., et al. (2000). Influence of mutation type and X chromosome inactivation on Rett syndrome phenotypes. Ann Neurol 47, 670-679.

Amir, R.E., Van den Veyver, I.B., Wan, M., Tran, C.Q., Francke, U., and Zoghbi, H.Y. (1999). Rett syndrome is caused by mutations in X-linked MECP2, encoding methyl-CpG-binding protein 2. Nat Genet 23, 185-188.

Asaka, Y., Jugloff, D.G., Zhang, L., Eubanks, J.H., and Fitzsimonds, R.M. (2006). Hippocampal synaptic plasticity is impaired in the Mecp2-null mouse model of Rett syndrome. Neurobiol Dis 21, 217-227.

Bauman, M.L., Kemper, T.L., and Arin, D.M. (1995). Pervasive neuroanatomic abnormalities of the brain in three cases of Rett's syndrome. Neurology 45, 1581-1586.

Belichenko, P.V., Hagberg, B., and Dahlstrom, A. (1997). Morphological study of neocortical areas in Rett syndrome. Acta Neuropathol 93, 50-61.

Belichenko, P.V., Wright, E.E., Belichenko, N.P., Masliah, E., Li, H.H., Mobley, W.C., and Francke, U. (2009). Widespread changes in dendritic and axonal morphology in Mecp2-mutant mouse models of Rett syndrome: evidence for disruption of neuronal networks. J Comp Neurol 514, 240-258.

Blackman, M.P., Djukic, B., Nelson, S.B., and Turrigiano, G.G. (2012). A Critical and Cell-Autonomous Role for MeCP2 in Synaptic Scaling Up. Journal of Neuroscience 32, 13529-13536.

Blochl, A., and Thoenen, H. (1996). Localization of cellular storage compartments and sites of constitutive and activity-dependent release of nerve growth factor (NGF) in primary cultures of hippocampal neurons. Mol Cell Neurosci 7, 173-190.

Bouzioukh, F., Daoudal, G., Falk, J., Debanne, D., Rougon, G., and Castellani, V. (2006). Semaphorin3A regulates synaptic function of differentiated hippocampal neurons. Eur J Neurosci 23, 2247-2254.

Brigadski, T., Hartmann, M., and Lessmann, V. (2005). Differential vesicular targeting and time course of synaptic secretion of the mammalian neurotrophins. J Neurosci 25, 7601-7614.

Cadigan, K.M., Fish, M.P., Rulifson, E.J., and Nusse, R. (1998). Wingless repression of Drosophila frizzled 2 expression shapes the Wingless morphogen gradient in the wing. Cell 93, 767-777.

Cazorla, M., Premont, J., Mann, A., Girard, N., Kellendonk, C., and Rognan, D. (2011). Identification of a low-molecular weight TrkB antagonist with anxiolytic and antidepressant activity in mice. J Clin Invest 121, 1846-1857.

Chahrour, M., Jung, S.Y., Shaw, C., Zhou, X., Wong, S.T., Qin, J., and Zoghbi, H.Y. (2008). MeCP2, a key contributor to neurological disease, activates and represses transcription. Science 320, 1224-1229.

Chang, Q., Khare, G., Dani, V., Nelson, S., and Jaenisch, R. (2006). The disease progression of Mecp2 mutant mice is affected by the level of BDNF expression. Neuron 49, 341-348.

Chao, H.T., Chen, H., Samaco, R.C., Xue, M., Chahrour, M., Yoo, J., Neul, J.L., Gong, S., Lu, H.C., Heintz, N., et al. (2010). Dysfunction in GABA signalling mediates autism-like stereotypies and Rett syndrome phenotypes. Nature 468, 263-269.

Chao, H.T., Zoghbi, H.Y., and Rosenmund, C. (2007). MeCP2 controls excitatory synaptic strength by regulating glutamatergic synapse number. Neuron 56, 58-65.

Chen, R.Z., Akbarian, S., Tudor, M., and Jaenisch, R. (2001). Deficiency of methyl-CpG binding protein-2 in CNS neurons results in a Rett-like phenotype in mice. Nat Genet 27, 327-331.

Chen, W.G., Chang, Q., Lin, Y., Meissner, A., West, A.E., Griffith, E.C., Jaenisch, R., and Greenberg, M.E. (2003). Derepression of BDNF transcription involves calcium-dependent phosphorylation of MeCP2. Science 302, 885-889.

Cheng, P.L., Song, A.H., Wong, Y.H., Wang, S., Zhang, X., and Poo, M.M. (2011). Self-amplifying autocrine actions of BDNF in axon development. Proc Natl Acad Sci U S A 108, 18430-18435.

Cohen, S., Gabel, H.W., Hemberg, M., Hutchinson, A.N., Sadacca, L.A., Ebert, D.H., Harmin, D.A., Greenberg, R.S., Verdine, V.K., Zhou, Z., et al. (2011).

Genome-wide activity-dependent MeCP2 phosphorylation regulates nervous system development and function. Neuron 72, 72-85.

Collins, A.L., Levenson, J.M., Vilaythong, A.P., Richman, R., Armstrong, D.L., Noebels, J.L., David Sweatt, J., and Zoghbi, H.Y. (2004). Mild overexpression of MeCP2 causes a progressive neurological disorder in mice. Hum Mol Genet 13, 2679-2689.

Dani, V.S., Chang, Q., Maffei, A., Turrigiano, G.G., Jaenisch, R., and Nelson, S.B. (2005). Reduced cortical activity due to a shift in the balance between excitation and inhibition in a mouse model of Rett syndrome. Proc Natl Acad Sci U S A 102, 12560-12565.

De Wit, J., De Winter, F., Klooster, J., and Verhaagen, J. (2005). Semaphorin 3A displays a punctate distribution on the surface of neuronal cells and interacts with proteoglycans in the extracellular matrix. Mol Cell Neurosci 29, 40-55.

de Wit, J., Toonen, R.F., and Verhage, M. (2009). Matrix-dependent local retention of secretory vesicle cargo in cortical neurons. J Neurosci 29, 23-37.

Degano, A.L., Pasterkamp, R.J., and Ronnett, G.V. (2009). MeCP2 deficiency disrupts axonal guidance, fasciculation, and targeting by altering Semaphorin 3F function. Mol Cell Neurosci 42, 243-254.

Deng, V., Matagne, V., Banine, F., Frerking, M., Ohliger, P., Budden, S., Pevsner, J., Dissen, G.A., Sherman, L.S., and Ojeda, S.R. (2007). FXYD1 is an MeCP2 target gene overexpressed in the brains of Rett syndrome patients and Mecp2-null mice. Hum Mol Genet 16, 640-650.

Deogracias, R., Yazdani, M., Dekkers, M.P.J., Guy, J., Ionescu, M.C.S., Vogt, K.E., and Barde, Y.A. (2012). Fingolimod, a sphingosine-1 phosphate receptor

modulator, increases BDNF levels and improves symptoms of a mouse model of Rett syndrome. Proceedings of the National Academy of Sciences of the United States of America 109, 14230-14235.

Desai, N.S., Rutherford, L.C., and Turrigiano, G.G. (1999). Plasticity in the intrinsic excitability of cortical pyramidal neurons. Nat Neurosci 2, 515-520.

Finsterwald, C., Fiumelli, H., Cardinaux, J.R., and Martin, J.L. (2010). Regulation of dendritic development by BDNF requires activation of CRTC1 by glutamate. J Biol Chem 285, 28587-28595.

Gabel, H.W., Kinde, B., Stroud, H., Gilbert, C.S., Harmin, D.A., Kastan, N.R., Hemberg, M., Ebert, D.H., and Greenberg, M.E. (2015). Disruption of DNA-methylation-dependent long gene repression in Rett syndrome. Nature 522, 89-93.

Gauthier, L.R., Charrin, B.C., Borrell-Pages, M., Dompierre, J.P., Rangone, H., Cordelieres, F.P., De Mey, J., MacDonald, M.E., Lessmann, V., Humbert, S., et al. (2004). Huntingtin controls neurotrophic support and survival of neurons by enhancing BDNF vesicular transport along microtubules. Cell 118, 127-138.

Giacometti, E., Luikenhuis, S., Beard, C., and Jaenisch, R. (2007). Partial rescue of MeCP2 deficiency by postnatal activation of MeCP2. Proc Natl Acad Sci U S A 104, 1931-1936.

Gottmann, K., Mittmann, T., and Lessmann, V. (2009). BDNF signaling in the formation, maturation and plasticity of glutamatergic and GABAergic synapses. Exp Brain Res 199, 203-234.

Guy, J., Gan, J., Selfridge, J., Cobb, S., and Bird, A. (2007). Reversal of neurological defects in a mouse model of Rett syndrome. Science 315, 1143-1147.

Guy, J., Hendrich, B., Holmes, M., Martin, J.E., and Bird, A. (2001). A mouse Mecp2-null mutation causes neurological symptoms that mimic Rett syndrome. Nat Genet 27, 322-326.

Hagberg, B., Aicardi, J., Dias, K., and Ramos, O. (1983). A progressive syndrome of autism, dementia, ataxia, and loss of purposeful hand use in girls: Rett's syndrome: report of 35 cases. Ann Neurol 14, 471-479.

Hung, M.S., and Shen, C.K. (2003). Eukaryotic methyl-CpG-binding domain proteins and chromatin modification. Eukaryot Cell 2, 841-846.

Jang, S.W., Liu, X., Yepes, M., Shepherd, K.R., Miller, G.W., Liu, Y., Wilson, W.D., Xiao, G., Blanchi, B., Sun, Y.E., et al. (2010). A selective TrkB agonist with potent neurotrophic activities by 7,8-dihydroxyflavone. Proc Natl Acad Sci U S A 107, 2687-2692.

Jentarra, G.M., Olfers, S.L., Rice, S.G., Srivastava, N., Homanics, G.E., Blue, M., Naidu, S., and Narayanan, V. (2010). Abnormalities of cell packing density and dendritic complexity in the MeCP2 A140V mouse model of Rett syndrome/ X-linked mental retardation. BMC Neurosci 11, 19.

Jiang, M., Ash, R.T., Baker, S.A., Suter, B., Ferguson, A., Park, J., Rudy, J., Torsky, S.P., Chao, H.T., Zoghbi, H.Y., et al. (2013). Dendritic arborization and spine dynamics are abnormal in the mouse model of MECP2 duplication syndrome. J Neurosci 33, 19518-19533.

Johnson, R.A., Lam, M., Punzo, A.M., Li, H., Lin, B.R., Ye, K., Mitchell, G.S., and Chang, Q. (2012). 7,8-dihydroxyflavone exhibits therapeutic efficacy in a mouse model of Rett syndrome. J Appl Physiol (1985) 112, 704-710.

Jordan, C., Li, H.H., Kwan, H.C., and Francke, U. (2007). Cerebellar gene expression profiles of mouse models for Rett syndrome reveal novel MeCP2 targets. BMC Med Genet 8, 36.

Jugloff, D.G., Jung, B.P., Purushotham, D., Logan, R., and Eubanks, J.H. (2005). Increased dendritic complexity and axonal length in cultured mouse cortical neurons overexpressing methyl-CpG-binding protein MeCP2. Neurobiol Dis 19, 18-27.

Jugloff, D.G., Vandamme, K., Logan, R., Visanji, N.P., Brotchie, J.M., and Eubanks, J.H. (2008). Targeted delivery of an Mecp2 transgene to forebrain neurons improves the behavior of female Mecp2-deficient mice. Hum Mol Genet 17, 1386-1396.

Kang, H., and Schuman, E.M. (1996). A requirement for local protein synthesis in neurotrophin-induced hippocampal synaptic plasticity. Science 273, 1402-1406.

Kishi, N., and Macklis, J.D. (2010). MeCP2 functions largely cell-autonomously, but also non-cell-autonomously, in neuronal maturation and dendritic arborization of cortical pyramidal neurons. Experimental Neurology 222, 51-58.

Kleschevnikov, A.M., Belichenko, P.V., Villar, A.J., Epstein, C.J., Malenka, R.C., and Mobley, W.C. (2004). Hippocampal long-term potentiation suppressed by increased inhibition in the Ts65Dn mouse, a genetic model of Down syndrome. J Neurosci 24, 8153-8160.

Kline, D.D., Ogier, M., Kunze, D.L., and Katz, D.M. (2010). Exogenous brain-derived neurotrophic factor rescues synaptic dysfunction in Mecp2-null mice. J Neurosci 30, 5303-5310.

Kohara, K., Yasuda, H., Huang, Y., Adachi, N., Sohya, K., and Tsumoto, T. (2007). A local reduction in cortical GABAergic synapses after a loss of endogenous brain-derived neurotrophic factor, as revealed by single-cell gene knock-out method. J Neurosci 27, 7234-7244.

Kolarow, R., Brigadski, T., and Lessmann, V. (2007). Postsynaptic secretion of BDNF and NT-3 from hippocampal neurons depends on calcium calmodulin kinase II signaling and proceeds via delayed fusion pore opening. J Neurosci 27, 10350-10364.

Kondo, M., Gray, L.J., Pelka, G.J., Christodoulou, J., Tam, P.P., and Hannan, A.J. (2008). Environmental enrichment ameliorates a motor coordination deficit in a mouse model of Rett syndrome--Mecp2 gene dosage effects and BDNF expression. Eur J Neurosci 27, 3342-3350.

Kovalchuk, Y., Holthoff, K., and Konnerth, A. (2004). Neurotrophin action on a rapid timescale. Curr Opin Neurobiol 14, 558-563.

Kron, M., Lang, M., Adams, I.T., Sceniak, M., Longo, F., and Katz, D.M. (2014). A BDNF loop-domain mimetic acutely reverses spontaneous apneas and respiratory abnormalities during behavioral arousal in a mouse model of Rett syndrome. Dis Model Mech 7, 1047-1055.

Larimore, J.L., Chapleau, C.A., Kudo, S., Theibert, A., Percy, A.K., and Pozzo-Miller, L. (2009). Bdnf overexpression in hippocampal neurons prevents dendritic atrophy caused by Rett-associated MECP2 mutations. Neurobiol Dis 34, 199-211.

Lessmann, V., Gottmann, K., and Malcangio, M. (2003). Neurotrophin secretion: current facts and future prospects. Prog Neurobiol 69, 341-374.

Levine, E.S., Crozier, R.A., Black, I.B., and Plummer, M.R. (1998). Brain-derived neurotrophic factor modulates hippocampal synaptic transmission by increasing N-methyl-D-aspartic acid receptor activity. Proc Natl Acad Sci U S A 95, 10235-10239.

Li, H., Zhong, X., Chau, K.F., Williams, E.C., and Chang, Q. (2011). Loss of activity-induced phosphorylation of MeCP2 enhances synaptogenesis, LTP and spatial memory. Nat Neurosci 14, 1001-1008.

Li, W., Calfa, G., Larimore, J., and Pozzo-Miller, L. (2012). Activity-dependent BDNF release and TRPC signaling is impaired in hippocampal neurons of Mecp2 mutant mice. Proc Natl Acad Sci U S A 109, 17087-17092.

Liyanage, V.R., and Rastegar, M. (2014). Rett syndrome and MeCP2. Neuromolecular Med 16, 231-264.

Lois, C., Hong, E.J., Pease, S., Brown, E.J., and Baltimore, D. (2002). Germline transmission and tissue-specific expression of transgenes delivered by lentiviral vectors. Science 295, 868-872.

Lonetti, G., Angelucci, A., Morando, L., Boggio, E.M., Giustetto, M., and Pizzorusso, T. (2010). Early environmental enrichment moderates the behavioral and synaptic phenotype of MeCP2 null mice. Biol Psychiatry 67, 657-665.

Lu, Y., Christian, K., and Lu, B. (2008). BDNF: a key regulator for protein synthesis-dependent LTP and long-term memory? Neurobiol Learn Mem 89, 312-323.

Luikenhuis, S., Giacometti, E., Beard, C.F., and Jaenisch, R. (2004). Expression of MeCP2 in postmitotic neurons rescues Rett syndrome in mice. Proc Natl Acad Sci U S A 101, 6033-6038.

Martinowich, K., Hattori, D., Wu, H., Fouse, S., He, F., Hu, Y., Fan, G., and Sun, Y.E. (2003). DNA methylation-related chromatin remodeling in activity-dependent BDNF gene regulation. Science 302, 890-893.

Massa, S.M., Yang, T., Xie, Y., Shi, J., Bilgen, M., Joyce, J.N., Nehama, D., Rajadas, J., and Longo, F.M. (2010). Small molecule BDNF mimetics activate TrkB signaling and prevent neuronal degeneration in rodents. J Clin Invest 120, 1774-1785.

Matsumoto, T., Rauskolb, S., Polack, M., Klose, J., Kolbeck, R., Korte, M., and Barde, Y.A. (2008). Biosynthesis and processing of endogenous BDNF: CNS neurons store and secrete BDNF, not pro-BDNF. Nat Neurosci 11, 131-133.

Mattson, M.P. (2008). Glutamate and neurotrophic factors in neuronal plasticity and disease. Ann N Y Acad Sci 1144, 97-112.

McAllister, A.K., Katz, L.C., and Lo, D.C. (1999). Neurotrophins and synaptic plasticity. Annu Rev Neurosci 22, 295-318.

McGraw, C.M., Samaco, R.C., and Zoghbi, H.Y. (2011). Adult neural function requires MeCP2. Science 333, 186.

Nan, X., and Bird, A. (2001). The biological functions of the methyl-CpG-binding protein MeCP2 and its implication in Rett syndrome. Brain Dev 23 Suppl 1, S32-37.

Neher, E., and Sakaba, T. (2008). Multiple roles of calcium ions in the regulation of neurotransmitter release. Neuron 59, 861-872.

Nguyen, M.V., Du, F., Felice, C.A., Shan, X., Nigam, A., Mandel, G., Robinson, J.K., and Ballas, N. (2012). MeCP2 is critical for maintaining mature neuronal

networks and global brain anatomy during late stages of postnatal brain development and in the mature adult brain. J Neurosci 32, 10021-10034.

Nuber, U.A., Kriaucionis, S., Roloff, T.C., Guy, J., Selfridge, J., Steinhoff, C., Schulz, R., Lipkowitz, B., Ropers, H.H., Holmes, M.C., et al. (2005). Up-regulation of glucocorticoid-regulated genes in a mouse model of Rett syndrome. Hum Mol Genet 14, 2247-2256.

Nuydens, R., Dispersyn, G., de Jong, M., van den Kieboom, G., Borgers, M., and Geerts, H. (1997). Aberrant tau phosphorylation and neurite retraction during NGF deprivation in PC12 cells. Biochem Biophys Res Commun 240, 687-691.

Ogier, M., Wang, H., Hong, E., Wang, Q., Greenberg, M.E., and Katz, D.M. (2007). Brain-derived neurotrophic factor expression and respiratory function improve after ampakine treatment in a mouse model of Rett syndrome. J Neurosci 27, 10912-10917.

Papkoff, J., and Schryver, B. (1990). Secreted int-1 protein is associated with the cell surface. Mol Cell Biol 10, 2723-2730.

Park, H., and Poo, M.M. (2013). Neurotrophin regulation of neural circuit development and function. Nat Rev Neurosci 14, 7-23.

Poduslo, J.F., and Curran, G.L. (1996). Permeability at the blood-brain and blood-nerve barriers of the neurotrophic factors: NGF, CNTF, NT-3, BDNF. Brain Res Mol Brain Res 36, 280-286.

Poo, M.M. (2001). Neurotrophins as synaptic modulators. Nat Rev Neurosci 2, 24-32.

Pruunsild, P., Kazantseva, A., Aid, T., Palm, K., and Timmusk, T. (2007). Dissecting the human BDNF locus: bidirectional transcription, complex splicing, and multiple promoters. Genomics 90, 397-406.

Rett, A. (1966). [On a unusual brain atrophy syndrome in hyperammonemia in childhood]. Wien Med Wochenschr 116, 723-726.

Rietveld, L., Stuss, D.P., McPhee, D., and Delaney, K.R. (2015). Genotype-specific effects of Mecp2 loss-of-function on morphology of Layer V pyramidal neurons in heterozygous female Rett syndrome model mice. Front Cell Neurosci 9, 145.

Rosenmund, C., and Stevens, C.F. (1996). Definition of the readily releasable pool of vesicles at hippocampal synapses. Neuron 16, 1197-1207.

Rossner, S., Ueberham, U., Schliebs, R., Perez-Polo, J.R., and Bigl, V. (1998). Neurotrophin binding to the p75 neurotrophin receptor is necessary but not sufficient to mediate NGF-effects on APP secretion in PC-12 cells. J Neural Transm Suppl 54, 279-285.

Roux, J.C., Zala, D., Panayotis, N., Borges-Correia, A., Saudou, F., and Villard, L. (2012). Unexpected link between Huntington disease and Rett syndrome. M S-Medecine Sciences 28, 44-46.

Roux, P.P., Bhakar, A.L., Kennedy, T.E., and Barker, P.A. (2001). The p75 neurotrophin receptor activates Akt (protein kinase B) through a phosphatidylinositol 3-kinase-dependent pathway. J Biol Chem 276, 23097-23104.

Sahay, A., Kim, C.H., Sepkuty, J.P., Cho, E., Huganir, R.L., Ginty, D.D., and Kolodkin, A.L. (2005). Secreted semaphorins modulate synaptic transmission in the adult hippocampus. J Neurosci 25, 3613-3620.

Schmid, D.A., Yang, T., Ogier, M., Adams, I., Mirakhur, Y., Wang, Q., Massa, S.M., Longo, F.M., and Katz, D.M. (2012). A TrkB small molecule partial agonist rescues TrkB phosphorylation deficits and improves respiratory function in a mouse model of Rett syndrome. J Neurosci 32, 1803-1810.

Shahbazian, M., Young, J., Yuva-Paylor, L., Spencer, C., Antalffy, B., Noebels, J., Armstrong, D., Paylor, R., and Zoghbi, H. (2002). Mice with truncated MeCP2 recapitulate many Rett syndrome features and display hyperacetylation of histone H3. Neuron 35, 243-254.

Sohal, V.S., Zhang, F., Yizhar, O., and Deisseroth, K. (2009). Parvalbumin neurons and gamma rhythms enhance cortical circuit performance. Nature 459, 698-702.

Tian, L., Guo, R., Yue, X., Lv, Q., Ye, X., Wang, Z., Chen, Z., Wu, B., Xu, G., and Liu, X. (2012). Intranasal administration of nerve growth factor ameliorate beta-amyloid deposition after traumatic brain injury in rats. Brain Res 1440, 47-55.

Tolwani, R.J., Buckmaster, P.S., Varma, S., Cosgaya, J.M., Wu, Y., Suri, C., and Shooter, E.M. (2002). BDNF overexpression increases dendrite complexity in hippocampal dentate gyrus. Neuroscience 114, 795-805.

Tropea, D., Giacometti, E., Wilson, N.R., Beard, C., McCurry, C., Fu, D.D., Flannery, R., Jaenisch, R., and Sur, M. (2009). Partial reversal of Rett Syndrome-like symptoms in MeCP2 mutant mice. Proc Natl Acad Sci U S A 106, 2029-2034.

Van Esch, H., Bauters, M., Ignatius, J., Jansen, M., Raynaud, M., Hollanders, K., Lugtenberg, D., Bienvenu, T., Jensen, L.R., Gecz, J., et al. (2005). Duplication of the MECP2 region is a frequent cause of severe mental

retardation and progressive neurological symptoms in males. Am J Hum Genet 77, 442-453.

Wadel, K., Neher, E., and Sakaba, T. (2007). The coupling between synaptic vesicles and Ca2+ channels determines fast neurotransmitter release. Neuron 53, 563-575.

Wan, M., Lee, S.S., Zhang, X., Houwink-Manville, I., Song, H.R., Amir, R.E., Budden, S., Naidu, S., Pereira, J.L., Lo, I.F., et al. (1999). Rett syndrome and beyond: recurrent spontaneous and familial MECP2 mutations at CpG hotspots. Am J Hum Genet 65, 1520-1529.

Wang, H., Chan, S.A., Ogier, M., Hellard, D., Wang, Q., Smith, C., and Katz, D.M. (2006). Dysregulation of brain-derived neurotrophic factor expression and neurosecretory function in Mecp2 null mice. J Neurosci 26, 10911-10915.

Wang, L., Chang, X., She, L., Xu, D., Huang, W., and Poo, M.M. (2015). Autocrine action of BDNF on dendrite development of adult-born hippocampal neurons. J Neurosci 35, 8384-8393.

Waterhouse, E.G., and Xu, B. (2009). New insights into the role of brain-derived neurotrophic factor in synaptic plasticity. Mol Cell Neurosci 42, 81-89.

Woo, N.H., Teng, H.K., Siao, C.J., Chiaruttini, C., Pang, P.T., Milner, T.A., Hempstead, B.L., and Lu, B. (2005). Activation of p75NTR by proBDNF facilitates hippocampal long-term depression. Nat Neurosci 8, 1069-1077.

Xiang, F., Buervenich, S., Nicolao, P., Bailey, M.E., Zhang, Z., and Anvret, M. (2000). Mutation screening in Rett syndrome patients. J Med Genet 37, 250-255.

Yang, F., Je, H.S., Ji, Y., Nagappan, G., Hempstead, B., and Lu, B. (2009). Pro-BDNF-induced synaptic depression and retraction at developing neuromuscular synapses. J Cell Biol 185, 727-741.

Yizhar, O., Fenno, L.E., Prigge, M., Schneider, F., Davidson, T.J., O'Shea, D.J., Sohal, V.S., Goshen, I., Finkelstein, J., Paz, J.T., et al. (2011). Neocortical excitation/inhibition balance in information processing and social dysfunction. Nature 477, 171-178.

Yoshii, A., and Constantine-Paton, M. (2010). Postsynaptic BDNF-TrkB signaling in synapse maturation, plasticity, and disease. Dev Neurobiol 70, 304-322.

Zhang, K., Osakada, Y., Vrljic, M., Chen, L., Mudrakola, H.V., and Cui, B. (2010). Single-molecule imaging of NGF axonal transport in microfluidic devices. Lab Chip 10, 2566-2573.

Zhang, X., and Poo, M.M. (2002). Localized synaptic potentiation by BDNF requires local protein synthesis in the developing axon. Neuron 36, 675-688.

Zhou, Z., Hong, E.J., Cohen, S., Zhao, W.N., Ho, H.Y., Schmidt, L., Chen, W.G., Lin, Y., Savner, E., Griffith, E.C., et al. (2006). Brain-specific phosphorylation of MeCP2 regulates activity-dependent Bdnf transcription, dendritic growth, and spine maturation. Neuron 52, 255-269.

Zuccato, C., Ciammola, A., Rigamonti, D., Leavitt, B.R., Goffredo, D., Conti, L., MacDonald, M.E., Friedlander, R.M., Silani, V., Hayden, M.R., et al. (2001). Loss of huntingtin-mediated BDNF gene transcription in Huntington's disease. Science 293, 493-498.

Zuccato, C., Marullo, M., Conforti, P., MacDonald, M.E., Tartari, M., and Cattaneo, E. (2008). Systematic assessment of BDNF and its receptor levels in human cortices affected by Huntington's disease. Brain Pathol 18, 225-238.

Appendix

1. Statement of Contributions

Unless stated otherwise, experiments have been performed by me. Imaging of hippocampal CA1 neuronal nuclei was done by Dr. Mayur Vadhvani and analysis of the same was done in collaboration with him. Experimental designs by Prof. Christian Rosenmund, Dr. Yuan-Ju Wu (for BDNF overexpression experiments) and me.

Preparation of astrocyte feeder cultures and microdot preparation was done by Annegret Felies and Rike Dannenberg. Sectioning of *Mecp2*$^{+/-}$ samples for neuronal nuclei analysis was done by Berit Soehl Kielczynski. Lentiviral constructs were designed by Dr. Thorsten Trimbuch and produced by Katja Poetschke, Bettina Brokowski and Carola Schweynoch. Animal genotyping for colony maintenance of *Mecp2*^{Tm2} and *MECP2*^{Tg1} lines were carried out by Sabine Lenz. The above mentioned are all members of the Rosenmund group.

2. Publications

- Loss of MeCP2 disrupts cell autonomous and autocrine BDNF signaling in mouse glutamatergic neurons. Sampathkumar et al., *eLife,* Oct 2016.

- Meyer, Sampathkumar et al., 2016; submitted to *Disease Models & Mechanisms*; manuscript under review.

- Neural stem cell culture model for LRRK2 function determines regulation of dopaminergic and microtubule-associated genes. Anne. K. Meyer, Charanya Sampathkumar, Lars Fransecky, Martina Maisel, Stefan Kissenkoetter, Grit Weselek, Sebastian Berndt, Matthias Kirsch, Johannes Schwarz, Andreas Hermann and Alexander Storch. *Basal Ganglia*, Volume 5, Nov 2015.

3. Poster Presentations

- *Role of MeCP2 in synapse formation and maintenance.* FENS-ESF International Conference "The Neurobiology of Synapses and their Dysfunction" (Stresa, Italy, August 2013)

- *Loss of MeCP2 affects normal development of hippocampal glutamatergic neurons by altering axonal and dendritic outgrowth.* Joint PhD retreat of the Helmholtz International Research School Molecular Neurobiology and the International Max-Planck Research School for Neuroscience (Berlin, Germany, September 2014)

- *A cell-autonomous role for BDNF in regulating neurite outgrowth and synapse formation in Mecp2$^{Null/y}$ hippocampal neurons.* SFB 665 International Symposium "Developmental disturbances in the CNS" (Berlin, Germany, September 2014)

- *Loss of MeCP2 affects normal development of hippocampal glutamatergic neurons.* Society for Neuroscience International Conference (Washington DC, USA, November 2014)

- *Role of BDNF signaling in synapse formation in Mecp2$^{Null/y}$ excitatory neurons.* Society for Neuroscience International Conference (Chicago, USA, October 2015)

- *A cell-autonomous role for BDNF in regulating synapse formation in Mecp2$^{Null/y}$ hippocampal glutamatergic neurons.* FENS Forum of Neuroscience (Copenhagen, Denmark, July 2016)

4. Conferences, workshops and meetings

- Helmholtz Soft Skills course “Research Skills Development” (Mainz, Germany, April 2012)
- Training course “Handling iPS cells” (Lund University, Sweden, October 2012)
- Helmholtz Soft Skills course “Presentation and Communication Skills” (Berlin, Germany, June 2013)
- FENS-ESF International Conference “The Neurobiology of Synapses and their Dysfunction” (Stresa, Italy, August 2013)
- Joint PhD retreat of the Helmholtz International Research School Molecular Neurobiology and the International Max-Planck Research School for Neuroscience (Berlin, Germany, September 2014)
- SFB 665 International Symposium “Developmental disturbances in the CNS” (Berlin, Germany, September 2014)
- Society for Neuroscience International Conference (Washington DC, USA, November 2014)
- Society for Neuroscience International Conference (Chicago, USA, October 2015)
- International Rare Disease Day Symposium (Berlin, Germany, February 2016)

- FENS Forum of Neuroscience (Copenhagen, Denmark, July 2016)

- SPARK Bioinnovations and Entrepreneurship Training Workshop (Stanford, USA, August 2016)